ISSN 0869-5911, Petrology, 2006, Vol. 14, No. 4, pp. 390–412. © Pleiades Publishing, Inc., 2006.
Original Russian Text © V.R. Vetrin, 2006, published in Petrologiya, 2006, Vol. 14, No. 4, pp. 415–438.

# Composition and Structure of the Lower Crust of the Belomorian Mobile Belt, Baltic Shield

**V. R. Vetrin**

*Geological Institute, Kola Science Center, Russian Academy of Sciences, ul. Fersmana 14, Apatity, Murmansk oblast, 184209 Russia*

*e-mail: vetrin@geoksc.apatity.ru*

Received April 29, 2005

**Abstract**—The lower crust of the Belomorian Mobile Belt consists predominantly of garnet peridotites with subordinate amounts of pyroxenites and spinel peridotites, which occur as xenoliths in Devonian diatremes and dikes in the southern part of the Kola Peninsula. When transported to the surface by ultrabasic melts, the xenoliths were affected by fluids from the host ultrabasic lamprophyres with the introduction of Ca, Mg, and such trace elements as Ba, Nb, Sr, and P. The concentrations of trace elements (Sm, Nd, Y, Ti, Zr, Ni, Cr, and others) and the Sm–Nd isotopic composition were not significantly modified, which makes it possible to use them to compare the xenoliths with the near-surface complexes and to reproduce the composition of the protoliths. The Paleoproterozoic lower crust was produced during the emplacement of mantle magmas into metabasites in the Neoarchean lower crust, a process that was accompanied by the contamination of the melts and the origin of rocks showing characteristics of mantle and crust material. The emplacement of significant melt volumes into the Neoarchean lower crust caused its heating and enabled its viscous–plastic flow. This flow could likely also affect the material of the upper mantle, as follows from the occurrence of spinel peridotite nodules among the garnet granulites with an increase in the amount of mantle xenoliths from the roof to bottom of the lower crust. The overall amount of ultrabasic rocks in the lower crust was evaluated at 8–10%.

**DOI:** 10.1134/S0869591106040047

## INTRODUCTION

There is still relatively little information on the lower continental crust of the Earth, with the rocks composing its discrete tectonic provinces differing in mineralogy, chemistry, metamorphic parameters, age, and genesis. Most researchers emphasize the differences between the compositions of the Precambrian and Phanerozoic lower crust: while the lowermost Phanerozoic crust contains much originally sedimentary rocks, the Precambrian lower crust is dominated by granulites whose protoliths were mafic magmatic derivatives (Downes, 1993; Rudnik and Fountain, 1995; Kempton et al., 1995).

The southern part of the Kola Peninsula is suitable for examining the lower parts of the Precambrian continental crust. This territory contains approximately 1000 explosion dikes and >40 explosion pipes, with some of them bearing xenoliths of deep rocks. Most of the explosion bodies are made up of 360- to 380-Ma ultrabasic lamprophyres, whose localization was controlled by the Kandalaksha graben of northwestern strike. This graben belongs to the Onega–Kandalaksha paleorift of the Belomorian rift system. The structures were formed in the Middle and Late Riphean and underwent reactivation in the Middle Paleozoic, when swarms of alkaline dikes, diatremes, and ring intrusions of alkaline–ultrabasic rocks and carbonatites were emplaced.

The earlier studies of the deep xenoliths in the area were focused on the compositions of their minerals and rocks and the crystallization sequences of the mineral assemblages. It was definitely established that the garnet granulites and some of the pyroxenites are fragments of lower crustal rocks (Shurkin and Rumyantseva, 1979; Sharkov and Pukhtel, 1987; Vetrin and Kalinkin, 1992; Neymark et al., 1993; Downes, 1993; Kempton et al., 1995). Later works within the scope of the EUROPROBE SVEKALAPKO international project expanded the area where xenoliths were found and provided newly obtained analytical data on their major- and trace-element compositions and on the U–Pb, Pb–Pb, Sm–Nd, and Ar–Ar isotopic system of the rocks and minerals. Xenoliths of garnet granulites were also found in kimberlite pipes in Archangelsk region (Markwick and Downes, 2000), eastern Finland (Hölttä et al., 2000), and agpaitic syenites of the Niva intrusion in the southwestern Kola Peninsula (Arzamastsev et al., 2000). The principal mineralogical and chemical features of the lower crustal xenoliths, their age, and the *P–T* conditions of their crystallization are reported in Table 1. Kimberlites in eastern Finland bear, along with lower crustal xenoliths, also nodules of spinel and garnet peridotites and diamondiferous eclogites from the upper mantle (Peltonen et al., 2002; Kukkonen and Peltonen, 1999).

**Table 1.** Modal and chemical composition, age, and *P–T* conditions of crystallization of lower crustal rocks in the Baltic Shield and the northern part of the East European Platform (based on the results of studying deep xenoliths)

| Locality and host rocks | Predominant rocks and their mineralogy | Chemistry of xenoliths | Age (Ga) and dating method | *P–T* parameters | Reference |
|---|---|---|---|---|---|
| Ultrabasic lamprophyres in the northwestern part of Kandalaksha Bay, Kola Peninsula | Garnet granulites (*Grt + Cpx + Pl ± Opx ± Qtz ± Kfs ± Phl ± Hbl ± Dol ± Cal*), pyroxenites (*Grt + Cpx ± Opx ± Hbl ± Qtz ± Dol ± Cal*), garnet–phlogopite–amphibole rocks (*Grt + Phl ± Hbl ± Opx ± Rt*) | Tholeiitic basalts, picrobasalts, and gabbro-anorthosites | 2.7–2.8; 2.4– 2.5; 1.7–1.8 (U–Pb), 2.0–2.8, maximum at 2.4–2.6 ($T_{Nd}$(DM)) | *P* = 12–15 kbar, *T* = 750–930°C | Sharkov and Puchtel, 1987; Vetrin and Kalinkin, 1992; Vetrin and Nemchin, 1998; Kempton et al., 1995, 2001; Koreshkova et al., 2001 |
| Agpaitic syenites, Niva intrusion, Kola Peninsula | Garnet granulites (*Grt + Cpx + Pl ± Hbl ± Bt*) | Metasomatized tholeiitic basalts | 2.7 (U–Pb) | *P* = 13.1–13.9 kbar, *T* = 750 ± 50°C | Arzamastsev et al., 2000 |
| Kimberlites of the Pachugskoe field, 60 km north of Archangelsk | Garnet granulites (*Grt ± Pl ± Cpx ± Scp ± Hbl ± Rt ± Ap*) | Subalkaline basalts | 1.7–1.9 ($T_{Nd}$(DM)) | *P* = 13.5–15.5 kbar, *T* = 670–730°C | Markwick and Downes, 2000 |
| Kimberlites, eastern Finland | Clinopyroxene–garnet–amphibole granulites (*Cpx + Hbl + Pl ± Grt ± Opx ± Bt*) | Tholeiitic basalts | 1.7–2.6 (U–Pb), 1.5–2.9 ($T_{Nd}$(DM)) | *P* = 7.5–12.5 kbar, *T* = 800–900°C | Hölttä et al., 2000 |

Note: Mineral symbols (Kretz, 1983): *Grt*—garnet, *Cpx*—clinopyroxene, *Pl*—plagioclase, *Opx*—orthopyroxene, *Qtz*—quartz, *Kfs*—potassic feldspar, *Phl*—phlogopite, *Bt*—biotite, *Hbl*—hornblende, *Dol*—dolomite, *Cal*—calcite, *Rt*—rutile, *Ap*—apatite, *Scp*—scapolite.

The lower crustal xenoliths are thought to be derivatives of high-Mg boninite-like melts metamorphosed to the granulite facies. They form a Paleoproterozoic province of 2.4- to 2.5-Ga magmatic rocks in the northern part of the Baltic Shield (Sharkov et al., 1999; Kempton et al., 2001). At the same time, the composition of the most thoroughly examined xenoliths from the Kandalaksha shore of the Kola Peninsula provides evidence that the sources of the protoliths of these xenoliths could have been more diverse, and these rocks can be similar not only to the coronites (drusites) and layered peridotite–pyroxenite–gabbronorite intrusions in this province but also to the basalts of Archean greenstone belts and gabbro-anorthosites (Vetrin and Kalinkin, 1992; Koreshkova et al., 2001).

These data highlight the urgency of identifying the composition of the protoliths of the lower crustal xenoliths with the use of geochemical and isotopic geochemical techniques. The results of our research indicate that the regional lower crust was formed in at least two major stages: Neoarchean and Paleoproterozoic. Our data on the velocities of seismic waves in the xenoliths demonstrate that these velocities are much lower than the $V_p$ and $V_s$ determined by seismic studies of the lower crust beneath the Baltic Shield (Grad and Luosto, 1987; Tripol'skii and Sharov, 2004). These discrepancies between the seismic wave velocities testify that the regional lower crust is heterogeneous, and the granulites include beds and lenses of denser and higher velocity rocks of ultrabasic composition, whose amount increases from the upper levels of the lower crust toward its bottom.

## GEOLOGY

Xenoliths of garnet granulites and pyroxenite were sampled in lamprophyre dikes and an explosion pipe exposed in islands of the Kandalaksha Archipelago, where they intrude tonalitic gneisses, granites, and amphibolites of the northeastern part of the Belomorian Mobile Belt. Belomorian rocks from our study area were dated at 2.67–2.73 Ga, and their Proterozoic metamorphism occurred at 1.9–1.7 Ga (Claesson et al., 2000). The lamprophyre dikes have northerly strikes (from 0°–40° to 330°), thicknesses of 0.5–1 m, and can be traced for up to 1 km. Their contacts with the host rocks are sharp, often with chill selvages in the inner contact zones. A monticellite kimberlite dike northeast of the town of Kandalaksha contains, along with garnet granulites and pyroxenites, nodules (1–3 cm across) of spinel peridotites (Vetrin and Kalinkin, 1992). Xenoliths are the most abundant and compositionally diverse in the explosion pipe exposed in Elovy Island. The pipe is oval in cross section (18 × 10.5 m) and was emplaced along the contact between granite-gneisses and garnet amphibolites (Fig. 1). The pipe is filled with volcanic breccia of angular fragments of the host granites and amphibolites (20–30%), rounded nodules of garnet granulites (40–50%), pyroxenites, hornblendites (5–10%), and a cementing mass corresponding to ultraba-

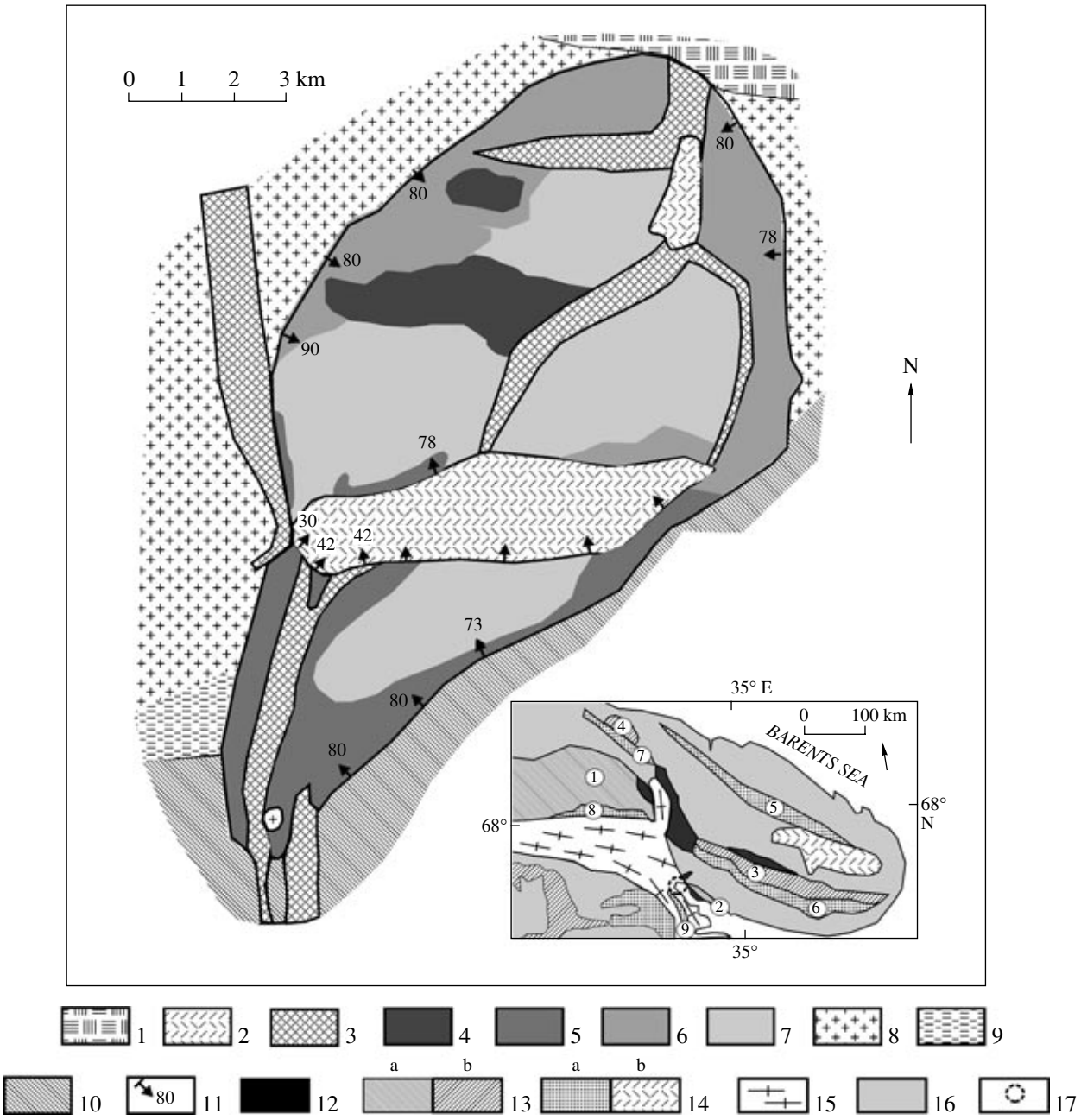


**Fig. 1.** Schematic geological maps of the diatreme in Elovy Island (modified after Shurkin and Rumyantseva, 1979) and the northeastern part of the Baltic Shield (inset).

(1) Quaternary deposits; (2) carbonatite; (3) ultrabasic lamprophyre; (4–7) breccia of the diatreme: (4) with rimmed xenoliths, (5) fine-grained, (6) medium-grained, (7) coarse-grained; (8) gneiss-granite; (9) granite-gneiss; (10) garnet amphibolite; (11) dips of contacts. Inset: (12) layered peridotite–pyroxenite–gabbronorite and gabbro–anorthosite intrusions; (13) Early Karelian belts and structures: (a) Lapland Granulite Belt, (b) paleorifts (circled numerals): (1) Sal'nye Tundry, (2) Kolvitsa, (3) Imandra–Varzuga, (4) Pechenga; (14) Late Archean structures: (a) greenstone belts (circled numerals): (5) Northern Kola, (6, 7) Terskii–Notozero (structures: 6—Terskii, Olenegorsk, Ingozero; 7—Kaskamskaya), (8) Korva Tundra structure; (9) Tikshozero belt; (b) Keivy paragneiss structure; (15) Belomorian Mobile Belt; (16) undifferentiated rocks of the Kola–Belomorian Complex and the basement complex; (17) study area.

sic lamprophyre in composition (10–20%). The garnet granulite nodules are 3–10, occasionally up to 40–60 cm across. The xenoliths of garnet granulites and pyroxenites are often rimmed with a fine-grained rock. If the nodules are small, the surrounding rims may be thicker than the nodules themselves. The K–Ar ages of the lamprophyres from the diatreme at Elovy Island and the dike at Srednii Sal'ny Island were estimated at 368 ± 15 and 360 ± 16 Ma, respectively, and the kimberlite dike was dated at 365 ± 16 Ma (Beard et al., 1998),

**Table 2.** Modal composition (%) of xenoliths

| Mineral | 37-30 | E/96-10(3) | E/96-10(1) | E/96-10(2) | 16/89 | 37-40 | 37-3(4) | 37-60 | 67-12 | 37-52 | 37-2 | 37-9(4) | 41-5 | 25-2 | 25-1(2) |
|---|---|---|---|---|---|---|---|---|---|---|---|---|---|---|---|
| | **1** | **2** | **3** | **4** | **5** | **6** | **7** | **8** | **9** | **10** | **11** | **12** | **13** | **14** | **15** |
| *Grt* | 12 | 35 | 25 | 20 | 44 | 22 | 20 | 30 | 38 | 30 | 42 | 8 | 10 | | |
| *Cpx* | 32 | 30 | 30 | 25 | 8 | 27 | 33 | 20 | 40 | 25 | 28 | 14 | 88 | 11 | 20 |
| *Opx* | 12 | | | | | + | 25 | | | | 1 | 74 | | 13 | |
| *Pl* | 40 | 25 | 25 | 50 | 37 | 44 | 15 | 40 | 20 | 35 | 20 | 1 | + | | |
| *Qtz* | | 5 | 5 | 5 | 3 | 3 | 3 | 2 | | 3 | 5 | | | | |
| *Kfs* | | | | | 1 | | | 3 | | 5 | 2 | | | | |
| *Hbl* | | | | | | + | + | | + | | + | | + | + | |
| *Ol* | | | | | | | | | | | | | | 73 | 74 |
| *Spl* | | | | | | | | | | | | | | 3 | 4 |
| *Phl* | + | + | + | + | | + | | | | + | | + | + | | + |
| *Rt* | | + | + | + | + | | 2 | + | | + | | | | | |
| *Mag* | 2 | | + | | + | + | | | | + | | 2 | | | |
| *Cal* | 2 | 5 | 5 | 3 | 4 | 4 | 2 | 5 | 2 | 2 | 2 | 6 | 2 | | 2 |
| *Scp* | | + | 10 | 2 | 3 | | | + | | | | | | | |
| *Ap* | | | | | | | | | | | | | | + | + |

Note: *Spl*—spinel, *Ol*—olivine, *Mag*—magnetite, other mineral symbols as in Table 1. Samples: (**1**–**11**) garnet granulites, (**12**, **13**) pyroxenites, (**14**, **15**) spinel peridotites. Empty cells correspond to the absence of the mineral.

which corresponds to the age of the Kola Paleozoic alkaline province (360–380 Ma; Kramm et al., 1993).

## MINERALOGY, *P–T* CONDITIONS OF CRYSTALLIZATION, AND AGE OF XENOLITHS

**Mineralogy.** The garnet granulites are medium-grained rocks, which consist mostly of garnet (20–50%), clinopyroxene (10–40%), plagioclase (15–50%), and orthopyroxene (0–25%), with all transitional types from mafic (eclogitic) to felsic varieties (Table 2). The contents of quartz, orthoclase, scapolite, and carbonates in the xenoliths usually do not exceed 3–5% for each of these minerals, and the rocks contain minor amounts of apatite, amphibole, zircon, monazite, rutile, aegirine, and magnetite. Single grains of carbonates and their aggregates fill interstices between mineral grains and cracks in them in the garnet granulites and occur as veinlets in xenoliths. Aluminous minerals (such as kyanite and sillimanite), which are typical of metasedimentary rocks, are completely absent from these rocks. These rocks usually have granoblastic, porphyroblastic, hypidioblastic, and, in places, cumulus and hypidiomorphic granular textures. The granulites often show taxitic, sometimes banded structures (Fig. 2), which are accentuated by discontinuous lamina of melanocratic (*Grt* + *Cpx* ± *Opx* ± *Pl*) and more leucocratic (*Pl* ± *Qtz*) composition and are in places migmatized. The processes of migmatization are petrographically expressed as the development of newly formed grains of plagioclase, orthoclase ($Or_{42}Ab_{49}An_9$), and quartz and the simultaneous decomposition and replacement of mafic rock-forming minerals of the garnet granulites. The rocks contain scarce xenoliths of phlogopite–garnet–orthopyroxene and amphibole–rutile–phlogopite–garnet rocks, which are thought to have been produced by the metasomatic recycling of the garnet granulites under the effect of fluids of mantle provenance (Bindeman et al., 1990; Vetrin and Kalinkin, 1992). These rocks are not considered in this publication.

The pyroxenites are two-pyroxene, amphibole–clinopyroxene, and garnet–clinopyroxene rocks. A xenolith of phlogopitized granulite is cut by veinlets of amphibole–clinopyroxene pyroxenite of massive structure, a fact suggesting that the origin of the regional lower crust was accompanied by a number of magmatic pulses.

The spinel peridotites consist of olivine (50–95%), clinopyroxene (0–15%), orthopyroxene (5–20%), and spinel (1–5%). The accessory minerals are amphibole, phlogopite, apatite, and picroilmenite, whose origin was related to the processes of modal mantle metasomatism. The rock shows traces of the percolation of mantle melts, which took place before the fragmentation of the spinel peridotites and the entrainment of xenoliths to the surface (Downes et al., 2000).

***P–T* conditions.** The crystallization temperatures of the mineral assemblages of the garnet granulites were

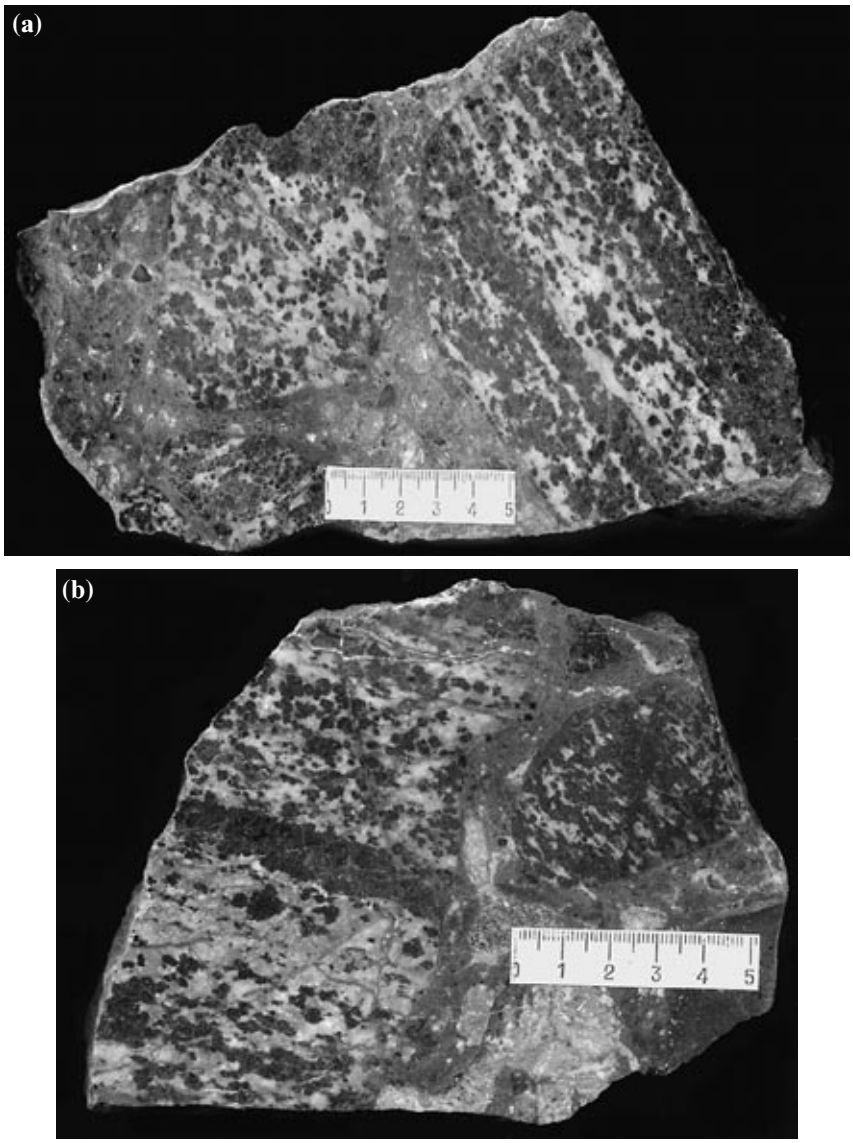


**Fig. 2.** Garnet granulites of (a) banded and (b) taxitic structure.

evaluated by the garnet–clinopyroxene geothermometer (Powell, 1985), and the pressures were estimated by the garnet–clinopyroxene–plagioclase–quartz geobarometer (Newton and Perkins, 1982; Powell and Holland, 1988). The values thus obtained ($T$ = 750–930°C, $P$ = 12–15 kbar; Kempton et al., 1995) demonstrate that the rocks affiliate with high-pressure granulites and were formed at depths of 30–45 km.

**Age of the mineral associations.** The U–Pb zircon dating of the granulites demonstrates that the same samples may sometimes contain zircons of Archean and Proterozoic age. Most zircon grains from sample 16/89 have an age of 1729 ± 29 Ma, but some grains have ages of 2.75 Ga (Vetrin, 1998). The ion-microprobe dating of single zircon grains from the garnet granulites (Downes et al., 2002) revealed that they included crystals of Paleoproterozoic age (2.47–2.41 and 1.77–1.61 Ga) and single grains of Archean age (2.84 Ga). Archean zircons were also identified in lower crustal xenoliths in the southwestern part of the Kola Peninsula (2711 ± 7 Ma; Arzamastsev et al., 2000) and eastern Finland (2.67–2.64 Ga; Hölttä et al., 2000), a fact suggesting that the Paleoproterozoic melts were contaminated with Archean crustal material. The results obtained on the U–Pb, Sm–Nd, and Ar–Ar isotopic system of the xenoliths point to the following stages of the origin and transformations of the lower crustal rocks in the Paleoproterozoic–Paleozoic:

2.5–2.4 Ga—emplacement of basic melts at the lower levels of the Late Archean crust and the crystallization of these melts under granulite-facies conditions (Neymark et al., 1993; Kempton et al., 2001; Downes et al., 2002);

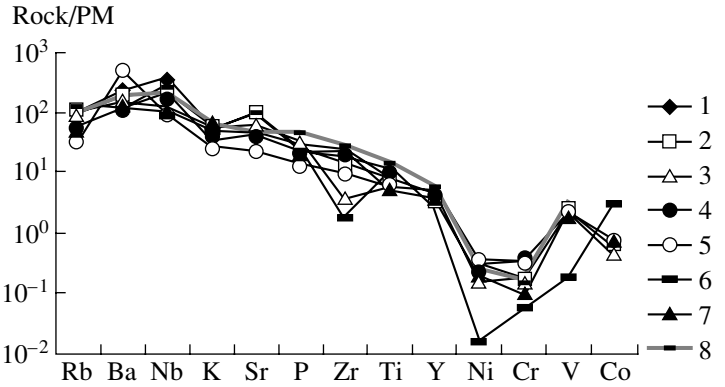


**Fig. 3.** Primitive mantle-normalized (Sun and McDonough, 1989) trace-element patterns for ultrabasic lamprophyres. (1–7) Numbers of analyses, same as in Table 2; (8) average composition of ultrabasic lamprophyres (Rock, 1991).

2.1–2.0 Ga—origin of the phlogopite (Kempton et al., 2001), emplacement of amphibole–clinopyroxene pyroxenite veins (Vetrin and Kalinkin, 1992; Kempton et al., 1995);

1.8–1.7 Ga—migmatization of the rocks (Vetrin and Nemchin, 1998), their partial melting, and the development of migmatites (Kempton et al., 1995);

0.43–0.39 Ga—alkaline metasomatism and the amphibolization of the lower crustal rocks before the emplacement of ultrabasic lamprophyre diatremes and dikes (Beard et al., 1996; Arzamastsev and Belyatskii, 1999; Vetrin and Travin, 2003).

### *Chemical Composition of Lamprophyres and Lower Crustal Xenoliths*

**The rocks from the diatreme at Elovy Island and dikes hosting the xenoliths** are undersaturated in silica (32.6–42.9 wt % $SiO_2$), rich in MgO, FeO, $Fe_2O_3$, $Na_2O$, and $K_2O$, have elevated mg# (0.63–0.73), and are thus similar to ultrabasic lamprophyres, according to the classification (Rock, 1991; Table 3). The ultrabasic lamprophyres from the diatreme contain, along with lower crustal xenoliths, also numerous nodules of the host granites and garnet amphibolites. When the melts were contaminated with granites, the composition of the ultrabasic lamprophyres changed, and these rocks became enriched in $SiO_2$, $Al_2O_3$, and $Na_2O$ and depleted in $Fe_2O_3$, FeO, MgO, CaO, and such trace elements as Ni, Cr, and V. The xenoliths are often surrounded by fine-grained rims [sample E/96-1(2)], whose composition is more melanocratic than that of lamprophyres from the pipe and close to the composition of the weakly contaminated ultrabasic lamprophyres from the dikes but differs from the latter in having higher concentrations of alkalis. The high concentrations of Cr, Ni (562 and 408 ppm on average, respectively), chemically bound $H_2O$, $CO_2$, and $P_2O_5$ suggest that the ultrabasic lamprophyres were produced by weakly fractionated mantle magma, which was saturated with fluids of $H_2O$–$CO_2$–phosphate composition. The lamprophyres are enriched in all incompatible elements with respect to the primitive mantle and have somewhat lower concentrations of P, Zr, Ti, and Y than those in the average ultrabasic lamprophyre (Rock, 1991) (Fig. 3). The depletion of these elements could be caused by both the higher degrees of mantle partial melting (than that of the average lamprophyre) during the derivation of the lamprophyres of the Kandalaksha shore and by the various degrees of differentiation of the melts, as well as by differences in the compositions of their sources and other factors. The clearly pronounced K minima in the multielemental patterns can, perhaps, be explained by the occurrence of a K-bearing phase (possibly, phlogopite) in the mantle residue.

During the crystallization of the host ultrabasic lamprophyres, the rocks of the xenoliths suffered active chemical alterations in the form of uneven carbonatization. Carbonate grains contained in these rocks in amounts of 2–6% consist of calcite and dolomite. The dolomite is an earlier mineral and occurs as individual grains (Table 4, sample 1) or relics of grains (sample 2) in the peripheral portions of calcite crystals (sample 3). The amount of carbonates (mostly calcite, sample 4) in the host rocks reaches 20–25%. Calcite occurs in these rocks as single anhedral grains or fills round globules up to 5 mm in diameter, which are located among minerals of the groundmass. The occurrence of carbonate veinlets that cut the xenoliths and continue into their host rocks testifies to the introduction of Ca, Mg, Sr, and P from the lamprophyres during the late magmatic stage of their crystallization. Assuming that the proportion of calcite and dolomite grains in the xenoliths are approximately equal to 1 to 2–3 and that all Ca, Mg, and Sr contained in the calcite and dolomite and their $CO_2$ were borrowed from the ultrabasic lamprophyres, the amount of CaO introduced into these xenoliths can be estimated at no less than 1–2 wt %, and the analogous estimates for MgO and SrO are 0.2–1 wt % and 10–40 ppm, respectively.

**The garnet granulites** of the xenoliths have $SiO_2$ concentrations varying from those corresponding to

**Table 3.** Concentrations of major (wt %) and trace (ppm) elements in ultrabasic lamprophyres

| Component | 50-4 | 38-1 | 19-7 | 67-4 | 52-1 | 37-1 | E/96-1(1) | E/96-1(2) | UBL |
|---|---|---|---|---|---|---|---|---|---|
| | **1** | **2** | **3** | **4** | **5** | **6** | **7** | **8** | **9** |
| $SiO_2$ | 32.58 | 34.09 | 35.35 | 36.27 | 37.95 | 37.30 | 42.95 | 32.56 | 32.3 |
| $TiO_2$ | 1.86 | 1.63 | 1.21 | 1.62 | 1.21 | 2.19 | 1.12 | 1.33 | 3.1 |
| $Al_2O_3$ | 6.46 | 7.09 | 9.07 | 5.72 | 7.03 | 7.78 | 9.46 | 7.64 | 6.7 |
| $Fe_2O_3$ | 5.86 | 6.40 | 6.34 | 6.60 | 7.03 | 3.25 | 2.69 | 5.36 | |
| FeO | 4.74 | 5.36 | 5.55 | 4.93 | 4.87 | 4.62 | 4.90 | 6.89 | 13.6 |
| MnO | 0.21 | 0.21 | 0.15 | 0.19 | 0.22 | 0.13 | 0.14 | 0.22 | 0.22 |
| MgO | 15.23 | 16.59 | 10.53 | 15.23 | 16.35 | 8.41 | 8.62 | 11.98 | 15.0 |
| CaO | 17.75 | 16.53 | 13.53 | 14.81 | 14.76 | 13.25 | 10.83 | 12.78 | 14.0 |
| $Na_2O$ | 0.84 | 1.95 | 3.25 | 0.95 | 0.56 | 3.57 | 3.95 | 1.96 | 1.0 |
| $K_2O$ | 1.65 | 1.52 | 1.72 | 0.98 | 0.75 | 1.67 | 1.42 | 2.63 | 1.9 |
| $H_2O^-$ | 0.31 | 0.26 | 0.78 | 1.03 | 0.48 | 0.58 | 0.91 | 0.74 | |
| $H_2O^+$ | 4.00 | 3.86 | 4.45 | 4.41 | 6.05 | 1.63 | 5.32 | 4.55 | 10.27 |
| $CO_2$ | 7.18 | 3.96 | 7.18 | 6.27 | 1.88 | 14.77 | 7.15 | 10.24 | |
| F | 0.34 | | 0.30 | 0.32 | 0.14 | | 0.18 | 0.30 | |
| $P_2O_5$ | 0.62 | 0.54 | 0.72 | 0.47 | 0.29 | 0.45 | 0.46 | 0.56 | 1.0 |
| Total | 99.49 | 99.99 | 99.70 | 99.32 | 99.52 | 99.60 | 100.02 | 99.74 | |
| mg # | 0.73 | 0.73 | 0.63 | 0.71 | 0.72 | 0.67 | 0.68 | 0.64 | 0.77 |
| Rb | 54 | 56 | 61 | 35 | 21 | 82 | 34 | | 65 |
| Ba | 1550 | 1250 | 1040 | 790 | 3360 | 800 | 840 | | 1110 |
| Nb | 261 | 150 | 82 | 137 | 66 | 210 | 74 | | 120 |
| Sr | 859 | 1990 | 1237 | 805 | 473 | 1870 | 1010 | | 950 |
| Zr | 244 | 152 | 40 | 205 | 106 | 20 | 242 | | 311 |
| Y | 21 | 16 | 17 | 18 | 16 | 12 | 18 | | 26 |
| Ni | 390 | 540 | 310 | 550 | 660 | 30 | 380 | | 430 |
| Co | 60 | 70 | 50 | 80 | 80 | 320 | 80 | | |
| Cr | 490 | 480 | 420 | 1100 | 1000 | 170 | 280 | | 480 |
| V | 200 | 190 | 160 | 180 | 180 | 15 | 140 | | 250 |

Note: (**1–8**) Ultrabasic lamprophyres: (**1–5**) from dikes, (**6–8**) from diatremes (**6**—fine-grained selvage around a xenolith), (**9**) average composition of ultrabasic lamprophyres (Rock, 1991). Major components were analyzed by the weight method, trace elements were determined by spectral analysis at the Geological Institute, Kola Science Center, Russian Academy of Sciences. Elements in empty cells were not determined.

picrobasalts to basaltic andesites with the predominance of rocks of basaltic composition (Table 5). The concentrations of $Al_2O_3$ in the granulites are usually 11–15 wt % and increase to 16–18 wt % in rocks enriched in plagioclase and containing the highest concentrations of alkalis (up to 6.7 wt % $Na_2O + K_2O$). The agpaitic coefficient [Na/(Al – K)] varies from 0.21 to 0.55 and determines the relatively low alkalinity of these rocks, with Na significantly dominating over K [Na/(Na + K) = 0.71–0.90]. The mg# values [Mg/(Mg + Fe*), where Fe* is total Fe] of the garnet granulites range from 0.46 to 0.63 and amount to 0.66–0.68 in the pyroxenites. According to their normative composition (Table 6), most of the xenoliths correspond to quartz tholeiites, with olivine tholeiites accounting for approximately one-third of the samples. Normative alsilite was detected only in two analyses of the garnet granulites, in which its concentrations did not exceed 4–7%. The two-pyroxene pyroxenites correspond to quartz tholeiites [sample 37-9(4)], and the garnet–clinopyroxene pyroxenites are analogues of alkaline basalts (sample 41-5).

Compared to the primitive mantle (Sun and McDonough, 1989), the xenoliths are enriched in incompatible elements but depleted in Ni and Cr (Table 5). Some xenoliths are characterized by high concentrations of Ba (up to 0.12–0.17 wt %), Nb (up to 25 ppm), Sr (up to 0.13 wt %), and $P_2O_5$ (up to 0.59 wt %). The host

lamprophyres bear Ba, Sr, and $P_2O_5$ concentrations comparable with those in the xenoliths but have higher contents of Nb. These data and the positive correlation of $CO_2$ with Ba, Nb, Sr, and $P_2O_5$ in the rocks (Fig. 4) suggest that these elements were introduced into the rocks owing to the contact effect of the ultrabasic melt on the xenoliths. Most trace elements (Sm, Nd, Y, Ti, Zr, Ni, Cr, Co, V, and Rb) are typically inert during carbonatization, or their concentrations slightly decrease with increasing $CO_2$ concentration and the associated carbonatization of the xenoliths (Fig. 4). The sums of the concentrations of REE in the garnet granulites are equal to 64–125 ppm, and the La concentrations are 36–88 times higher than the chondritic values, with the $(La/Yb)_n$ ratios varying from 4.4 to 16.9. When compared with the standard types of Archean and modern basalts (Condie, 1981), the REE composition of the garnet granulites is closer to that of the TH2 basalts of greenstone belts and differs from modern calc–alkaline basalts in having elevated concentrations of LREE and lower HREE (Fig. 5). A mineralogical control on the REE distribution in the granulites is weak and can possibly be pronounced only in an increase in the concentrations of HREE when the rocks are enriched in garnet (sample 16/89), the appearance of poorly pronounced Eu maximum (Eu/Eu* = 1.14) in the plagioclase granulite (sample 37-40), and the decrease in the concentrations of LREE in the two-pyroxene granulite [sample 37-3(4)].

The petrography and geochemistry of the xenoliths indicate that they are magmatic derivatives with normal or elevated alumina contents and relatively high sodium contents. In binary compositional diagrams, the garnet granulites display direct correlations between their mg# values and the composition of the normative plagioclase [$100An/(An + Ab)$, Fig. 6a] and the mg# values and the concentrations of Ni and Cr (Figs. 6b, 6c). The reasons for these correlations could be both the effect of crystallization differentiation of one or several parental magmas and changes in the composition of the melts during their contamination with Archean protocrustal material. In a mg#–$100An/(An + Ab)$ diagram, the data points of the pyroxenites plot separately from the compositional field of the garnet granulites, which seems to have been predetermined by the differences in the compositions of the parental melts of the granulites and pyroxenites.

## Sm–Nd ISOTOPIC SYSTEMATICS OF XENOLITHS

The garnet granulites and garnet–clinopyroxene pyroxenite (sample 41-5) have $^{147}Sm/^{144}Nd$ and $^{143}Nd/^{144}Nd$ ratios equal to 0.10006–0.15747 and 0.511194–0.511902, respectively (Table 7). The analogous ratios of the ultrabasic lamprophyres are 0.08505–0.09396 and 0.512116–0.512347, respectively, and, hence, the data points of these rocks and xenoliths define discrete fields in the upper and lower parts of the Sm–Nd diagram (Fig. 7). The absence of rocks with intermediate $^{147}Sm/^{144}Nd$ and $^{143}Nd/^{144}Nd$ ratios suggests that the Sm–Nd isotopic systems of the xenoliths were not modified any significantly when the xenoliths were entrained to the surface by the ultrabasic lamprophyre melts. All data points of the xenoliths in the Sm–Nd diagram can be approximated by an errorchron corresponding to an age of 1.65 ± 0.51 Ga, MSWD = 38.7. The significant dispersion of the isotopic ratios makes it difficult to interpret this value as the age of any geologically definite event pronounced in this territory. At the same time, two samples of the garnet granulites (samples 37-2 and 37-40) with the lowest $^{147}Sm/^{144}Nd$ and $^{143}Nd/^{144}Nd$ ratios, one sample of garnet pyroxenite (sample 41-5), and sample 16/89 yielded an isochron dependence corresponding to an age of 2480 ± 110 Ma, MSWD = 0.916. This age estimate is in good agreement with the age of the intrusive rocks and related volcanics of the Paleoproterozoic magmatic province in the Baltic Shield with an age of 2.5–2.4 Ga (Sharkov et al., 1999). The plausibility of this age estimate also follows from the ages of zircons (2.47–2.41 Ga; Downes et al., 2002) and feldspars (~2.4 Ga; Neymark et al., 1993; Kempton et al., 2001) from xenoliths collected in this territory.

The model age of the xenoliths recalculated according to the single-stage model varies from 2400 to 3365 Ma. As follows from Table 7, the oldest model age was obtained for the rocks whose $^{147}Sm/^{144}Nd$ ratios [up to 0.15747, sample E-96-10(3)] are higher than the average ratio assumed for the Earth's crust (0.12; Faure, 1986). Elevated $^{147}Sm/^{144}Nd$ ratios suggest that isotopic fractionation occurred after the separation of the protolith from the mantle, which allowed us to apply the two-stage model to constrain the age of these rocks. According to this model (Liew and Hofmann, 1988), the measured Sm/Nd ratios could be produced by some process, which can be dated by some independent

**Table 4.** Chemical composition (wt %) of carbonates from (1–3) xenoliths and (4) their host ultrabasic lamprophyre

| Component | 1 | 2 | 3 | 4 |
|---|---|---|---|---|
| | Dolomite, core | Dolomite, margin | Calcite, core | Calcite, core |
| CaO | 26.91 | 33.59 | 54.17 | 55.18 |
| MgO | 17.84 | 13.57 | 0.43 | 0.16 |
| FeO | 4.71 | 8.25 | 0.90 | 0.07 |
| SrO | | 0.08 | 0.08 | 0.09 |
| $CeO_2$ | | – | – | – |
| MnO | – | – | – | 0.16 |

Note: Analyses were conducted on an X-ray microprobe (analysts L.I. Polezhaeva and E.E. Savchenko, Geological Institute, Kola Science Center, Russian Academy of Sciences). Empty cells mean that the element was not analyzed, dashes mean dot detected.

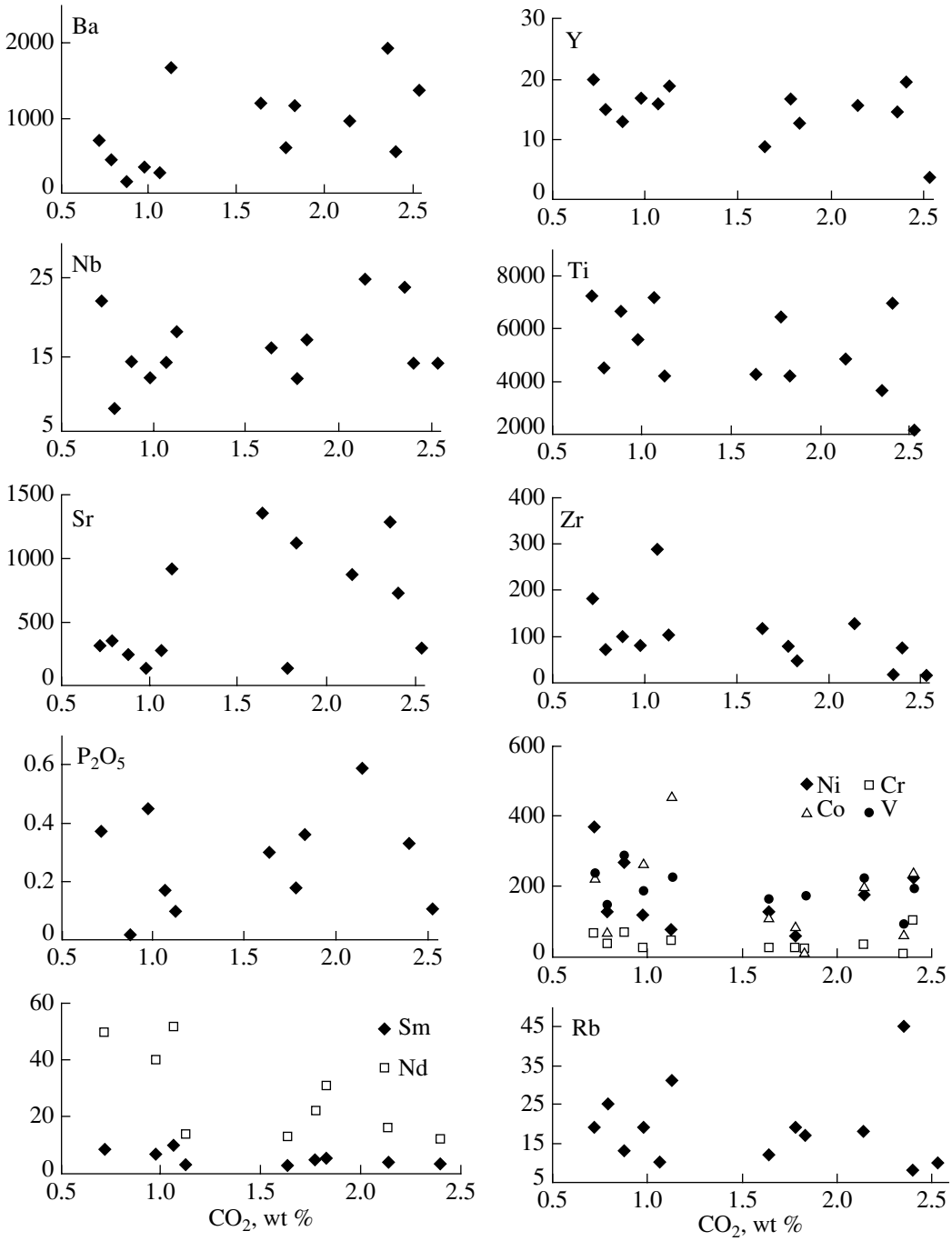


**Fig. 4.** Correlations between the concentrations of trace elements (ppm) and $CO_2$ in xenoliths.

method, and the $^{147}Sm/^{144}Nd$ ratio before this time can be assumed to have been close to the average crustal value. It was demonstrated in earlier publications (Neymark et al., 1993; Kempton et al., 2001) that isotopic equilibration in the Sm/Nd system of the xenoliths took place at approximately 1500 Ma. This enabled us to use this value to calculate the two-stage model age $T_{Nd}$(DM-2st) (Table 7). The results thus obtained highlight the age heterogeneity of the lower crustal protoliths, whose separation from the mantle occurred within the age interval of 2.94–2.55 Ga. These age values can be interpreted as an indication of the crustal prehistory of the xenoliths (at 2.94–2.45 Ga) and as evidence that the Paleoproterozoic melts were contaminated with Archean crustal material. The values of $\varepsilon_{Nd}$ of the xenoliths calculated for an age of 2.45 Ga varies from negative to positive values (from –2.5 to +2.15). It is known that negative $\varepsilon_{Nd}$ values of Paleoproterozoic

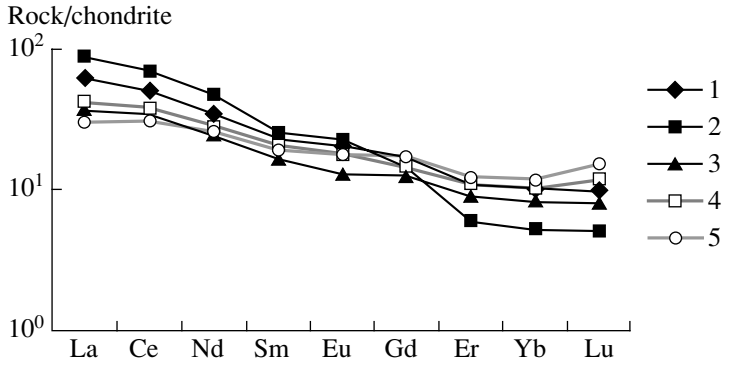


**Fig. 5.** Chondrite-normalized (Boynton, 1984) REE patterns for (1–3) garnet granulite xenoliths (Table 4, analyses 1–3), (4) tholeiites of Archean greenstone belts TH2, and (5) modern calc–alkaline basalts (Condie, 1981).

rocks are most typical of layered intrusions (Balashov et al., 1993; Amelin et al., 1995), coronites (Lobach-Zhuchenko et al., 1998), and gabbro-anorthosites (Balaganskii et al., 1998), which are thought to have been derived from an enriched source. The origin of some protoliths of the xenoliths in the Paleoproterozoic is confirmed by the fact that these rocks contain zircons with ages of 2.5–2.4 Ga. The reasons for the positive $\varepsilon_{Nd}$ values of the xenoliths could be as follows: (i) the protoliths could have been derived from a depleted mantle source, and (ii) the Paleoproterozoic melts could be contaminated with the material of the Archean crust. The first explanation is, however, at variance with the concentrations of REE, Zr, Ti, Y, Ni, and V in the xenoliths, which are comparable with the concentrations of these elements in xenoliths with negative $\varepsilon_{Nd}$ values (Table 5). At the same time, the process of contamination of the Paleoproterozoic melts with Archean crustal material is corroborated by the fact that the xenoliths contain zircons with ages of 2.84–2.6 Ga. The most probable contaminants of the Paleoproterozoic melts are the rock associations of the two major constituents of the Archean continental crust: rocks from high-grade metamorphic terranes and from granite–greenstone belts (Condie, 1981). One of the latter is the Belomorian Mobile Belt, which consists of large tectonic nappes. These nappes are fragments of the Karelian granite–greenstone terrane, which is situated south of our study area (Glebovitsky, 1993). The great depths at which the mineral assemblages of the xenoliths crystallized (30–45 km) make it hardly possible that the parental melts were contaminated with sedimentary rocks and granitoids of tonalite–trondhjemite composition, the major constituents of, respectively, terranes of Archean high-grade metamorphic and granite–greenstone rocks. The absence of metasediments from the regional lower crust follows from data on the petrography and petrochemistry of xenoliths. The most probable contaminants of the Paleoproterozoic melts could be deep-seated analogues of the Archean mafic volcanics, a concept consistent with the similarities between the REE patterns of the xenoliths and the basalts from typical greenstone belts worldwide (Fig. 5). Additional information on the possible composition of the rocks that contaminated the Paleoproterozoic melts can be obtained by studying the Sm–Nd isotopic systematics of the Archean granitoids and mafic rocks. In an age–$\varepsilon_{Nd}$ diagram (Fig. 8), the data points of the xenoliths with negative $\varepsilon_{Nd}$ values plot within the compositional field of layered intrusions in the Kola Peninsula, which is partly overlapped by the field of granitoids of tonalite–trondhjemite composition from Archean granite–greenstone belts (Timmerman and Daly, 1995; Vetrin et al., 2003). The data points of the xenoliths with positive $\varepsilon_{Nd}$ values plot within the field of basic volcanics from Archean greenstone belts in the Kola Peninsula (Vetrin et al., 2003; Vrevskii et al., 2003) and northern Karelia (Mil'kevich et al., 2003) whose isotopic composition is recalculated to an age of 2450 Ma. The similarities between the isotopic compositions of these rocks led us to believe that the basic metavolcanics should have been the main contaminant of the Paleoproterozoic melts. This diagram also demonstrates the low probability of the origin of rocks with positive $\varepsilon_{Nd}$ values via the contamination of the Paleoproterozoic melts with Archean granitoids.

## PHYSICAL CHARACTERISTICS OF XENOLITHS

Physical characteristics of xenoliths, first of all, their elastic properties and density, are significant because enable the researcher to compare these values with the results of regional deep seismic sounding with the aim of developing models for the deep structure of the regional crust. The physical characteristics of the lower crustal xenoliths were examined at the Laboratory of Geophysics, Geological Institute, Kola Research Center, Russian Academy of Sciences. These characteristics included the densities of the xenoliths and the velocities of longitudinal and transverse seismic waves in them under pressures ranging from atmospheric to 85 MPa. The measurements were conducted by S.B. Melezhik by the methods described in (Kobranova et al., 1977). The velocities of seismic waves in a

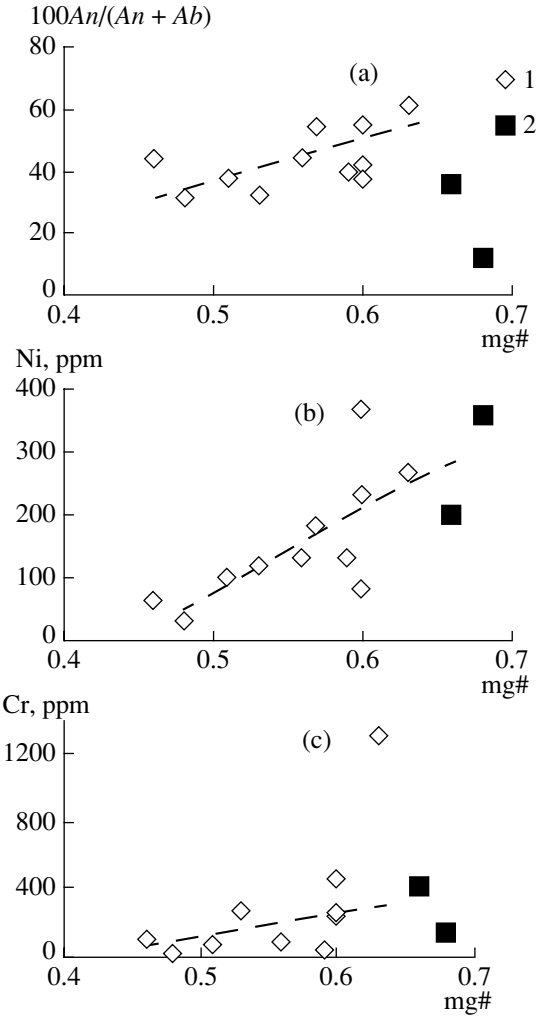


**Fig. 6.** Correlations between (a) 100*An*/(*Ab* + *An*) ratio and mg#, (b) Ni concentration and mg#, and (c) Cr concentration and mg# for xenoliths of (1) garnet granulites and (2) pyroxenites.

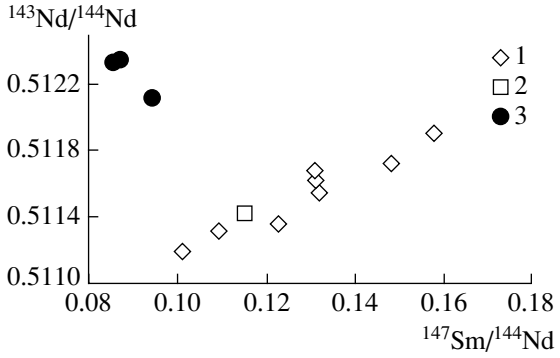


**Fig. 7.** $^{143}Nd/^{144}Nd$–$^{147}Sm/^{144}Nd$ diagram. (1) Garnet granulites; (2) pyroxenite; (3) ultrabasic lamprophyres.

garnet granulite sample under high pressures (up to 560 MPa) were measured by V.N. Korchin at the Subbotin Institute of Geophysics, National Academy of Sciences of Ukraine, following the methods described in (Lebedev et al., 1988).

The density of the garnet granulites and pyroxenites was measured at $P$ = 1 atm and $T$ = 20°C and ranged from 2.7 to 3.15 g/cm$^3$ (averaging 2.97 and 2.87 g/cm$^3$, respectively), which corresponds to the density of basic rocks: meso- and melanocratic gabbro, gabbro-norites, and garnet-bearing granulites (*Petrophysical…*, 1976). The average velocities of the longitudinal ($V_p$) and transverse ($V_s$) waves in the rocks of the xenoliths are 6.03 and 3.54 km/s, respectively, and display a clearly pronounced positive correlation with the densities of the rocks (Table 8, Fig. 9). The $\sigma$–$V_p$ and $\sigma$–$V_s$ regression lines have similar slopes, which determines a narrow range of the $V_p/V_s$ ratios equal to 1.71 ± 0.09. The velocities of longitudinal waves were measured in nine samples of the garnet granulites under pressures of up to 85 MPa. The $P$–$V_p$ lines (Fig. 10) of some of the samples are characterized by the steepest angles to the ordinate axis at pressures of up to 30–60 MPa, perhaps, due to an increase in the velocities in response to the closure of most pores in the rocks. The $V_p$ and $V_s$ values were measured under high pressures in a sample of garnet granulite [sample 67-8(3)] of the following composition: 60% *Cpx*, 30% *Grt*, and 10% *Pl*. These values at $P$ = 560 MPa were 6.48 and 3.76 km/s, respectively, and characterize the velocities of seismic waves in the pore-free rocks under the specified pressure. The increments $\Delta V_p$ and $\Delta V_s$ of the velocities for this sample over the whole specified range of pressures were, respectively, 0.46 and 0.21 km/s. When the values for the whole selection of samples (whose $V_p$ and $V_s$ were measured at $P$ = 1 atm and $T$ = 20°C) were extrapolated, using these values, to $P$ = 560 MPa, we obtained average values of $V_p$ = 6.49 km/s, $V_s$ = 3.75 km/s, and $V_p/V_s$ = 1.73. The calculated velocities of longitudinal and transverse waves are much lower than the analogous values for the lower crustal rocks of the Baltic Shield (7.23 and 4.13 km/s, respectively; Grad and Luosto, 1987) and for the lower continental crust as a whole (6.94 and 3.92 km/s; Rudnick and Fountain, 1995) for $T$ = 20°C and $P$ = 600 MPa, i.e., conditions close to those of our experiment.

## DISCUSSION

### *Comparison of the Composition of the Xenoliths and Subvolcanic Magmatic Complexes*

The materials obtained on the xenoliths demonstrate that the lower crustal rocks were affected by a succession of processes of variable ages: metamorphism to the granulite facies, granitization, phlogopitization, amphibolization, and contact metamorphism under the effect of the host lamprophyres. Inasmuch as our samples contained no more than 3–5% orthoclase and only single grains of amphibole and phlogopite, it is reasonable to believe that the processes of granitization,

**Table 5.** Concentrations of major (wt %) and trace (ppm) elements in xenoliths

| Component | 37-30 | E/96-10(3) | E/96-10(1) | E/96-10(2) | 16/89 | 37-40 | 37-3(4) | 37-60 | 67-12 | 37-52 | 37-2 | 37-9(4) | 41-5 | PM |
|---|---|---|---|---|---|---|---|---|---|---|---|---|---|---|
| | **1*** | **2** | **3** | **4** | **9*** | **7*** | **5*** | **10** | **8*** | **6** | **11*** | **12*** | **13*** | |
| $SiO_2$ | 44.22 | 46.67 | 47.33 | 51.62 | 49.93 | 51.45 | 52.09 | 52.15 | 52.95 | 53.50 | 54.51 | 46.08 | 48.19 | 44.9 |
| $TiO_2$ | 1.11 | 1.17 | 0.82 | 0.72 | 1.08 | 0.71 | 0.70 | 0.62 | 1.21 | 0.75 | 0.93 | 0.37 | 1.20 | 0.217 |
| $Al_2O_3$ | 10.71 | 14.73 | 13.46 | 16.91 | 18.46 | 18.06 | 14.59 | 16.73 | 13.53 | 15.18 | 15.11 | 4.54 | 7.79 | 4.63 |
| $Fe_2O_3$ | 5.06 | 4.65 | 3.87 | 2.29 | 3.10 | 3.40 | 2.16 | 3.24 | 1.43 | 2.63 | 1.53 | 6.64 | 4.38 | |
| FeO | 8.06 | 8.10 | 7.40 | 5.52 | 5.63 | 4.46 | 7.12 | 4.41 | 7.44 | 6.73 | 6.12 | 8.48 | 6.08 | 7.85 |
| MnO | 0.15 | 0.21 | 0.19 | 0.15 | 0.15 | 0.13 | 0.16 | 0.12 | 0.10 | 0.20 | 0.13 | 0.14 | 0.11 | 0.13 |
| MgO | 11.80 | 10.20 | 8.17 | 6.00 | 4.02 | 3.97 | 7.32 | 4.20 | 7.29 | 6.47 | 4.74 | 17.11 | 11.05 | 37.2 |
| CaO | 12.32 | 7.23 | 11.16 | 8.38 | 8.82 | 7.15 | 8.76 | 8.87 | 7.57 | 8.27 | 7.55 | 4.23 | 15.90 | 3.73 |
| $Na_2O$ | 1.50 | 1.77 | 2.32 | 3.96 | 4.01 | 5.67 | 3.79 | 3.82 | 3.08 | 3.28 | 4.07 | 0.93 | 2.62 | 0.369 |
| $K_2O$ | 0.47 | 0.63 | 0.85 | 1.26 | 1.29 | 0.99 | 0.86 | 2.41 | 1.06 | 1.18 | 2.05 | 0.31 | 0.17 | 0.03 |
| $H_2O^-$ | <0.05 | 0.45 | 0.06 | 0.09 | 0.20 | 0.11 | 0.20 | 0.13 | 0.59 | 0.10 | 0.10 | 2.81 | 0.08 | |
| $H_2O^+$ | 3.09 | 1.07 | 1.28 | 0.87 | 1.30 | 1.21 | 0.89 | 0.52 | 2.38 | 0.42 | 1.73 | 5.44 | 0.86 | |
| $CO_2$ | 0.88 | 2.40 | 2.14 | 1.64 | 1.78 | 1.83 | 1.13 | 2.35 | 0.72 | 0.79 | 0.98 | 2.53 | 1.07 | |
| F | 0.059 | 0.14 | 0.067 | 0.056 | 0.029 | 0.039 | 0.06 | 0.098 | 0.082 | 0.027 | 0.05 | 0.43 | 0.063 | |
| Cl | <0.01 | | | | 0.02 | 0.01 | 0.01 | | 0.01 | | | 0.01 | | |
| $P_2O_5$ | <0.05 | 0.33 | 0.59 | 0.30 | 0.18 | 0.36 | 0.10 | | 0.37 | | 0.45 | 0.11 | 0.17 | 0.022 |
| Total | 99.35 | 99.55 | 99.61 | 99.68 | 99.93 | 99.48 | 99.84 | 99.53 | 99.68 | 99.48 | 99.98 | 99.52 | 99.64 | |
| mg # | 0.63 | 0.60 | 0.57 | 0.59 | 0.46 | 0.48 | 0.60 | 0.51 | 0.60 | 0.56 | 0.53 | 0.68 | 0.66 | |
| *agp* | 0.24 | 0.21 | 0.30 | 0.42 | 0.39 | 0.55 | 0.45 | 0.44 | 0.41 | 0.39 | 0.52 | 0.36 | 0.57 | |
| *n* | 0.83 | 0.82 | 0.80 | 0.83 | 0.83 | 0.90 | 0.87 | 0.71 | 0.81 | 0.81 | 0.75 | 0.82 | 0.96 | |
| Rb | 13 | 8 | 18 | 12 | 19 | 17 | 31 | 45 | 19 | 25 | 19 | 10 | 10 | 0.635 |
| Ba | 150 | 570 | 990 | 1210 | 630 | 1190 | 1690 | 1950 | 700 | 440 | 340 | 140 | 270 | 6.99 |
| Nb | 14 | 14 | 25 | 16 | 12 | 17 | 18 | 24 | 22 | 8 | 12 | 14 | 14 | 0.713 |
| La | | | | | 19.11 | 27.39 | 11.28 | | | | | | | 0.687 |
| Ce | | | | | 40.51 | 56.05 | 27.28 | | | | | | | 1.78 |
| Sr | 238 | 731 | 878 | 1355 | 137 | 1120 | 915 | 1297 | 315 | 355 | 137 | 299 | 275 | 21.1 |
| Nd | | | | | 20.61 | 28.02 | 14.64 | | | | | | | 1.35 |
| Sm | | | | | 4.39 | 4.917 | 3.199 | | | | | | | 0.444 |
| Zr | 100 | 79 | 130 | 118 | 80 | 50 | 105 | 21 | 181 | 71 | 80 | 17 | 287 | 11.2 |
| Eu | | | | | 1.491 | 1.662 | 0.949 | | | | | | | 0.168 |
| Gd | | | | | 4.435 | 3.693 | 3.254 | | | | | | | 0.596 |
| Y | 13 | 20 | 16 | 9 | 17 | 13 | 19 | 15 | 20 | 15 | 17 | 4 | 16 | 4.55 |
| Er | | | | | 2.366 | 1.255 | 1.873 | | | | | | | 0.48 |
| Yb | | | | | 2.151 | 1.09 | 1.743 | | | | | | | 0.493 |
| Lu | | | | | 0.317 | 0.163 | 0.257 | | | | | | | 0.074 |
| Ni | 270 | 230 | 180 | 130 | 62 | 30 | 80 | 100 | 370 | 130 | 120 | 360 | 200 | 1890 |
| Co | 73 | 110 | 40 | 30 | 31 | 30 | 50 | 17 | 70 | 42 | 30 | 150 | 50 | 110 |
| Cr | 1300 | 250 | 210 | 120 | 94 | 20 | 460 | 74 | 230 | 76 | 270 | 140 | 400 | 2940 |
| V | 290 | 200 | 230 | 170 | 240 | 180 | 230 | 100 | 240 | 150 | 190 | 150 | 300 | 82 |

Note: (**1**–**11**) Garnet granulites; (**12**, **13**) garnet pyroxenites. Empty cells mean that the element was not analyzed. REE were analyzed by isotopic dilution at the Institute of the Geology of Ore Deposits, Petrography, Mineralogy, and Geochemistry, Russian Academy of Sciences (Kempton et al., 2001); mg# = $Mg/(Mg + Fe_{tot})$, *agp* = Na/(Al – K), *n* = Na/(Na + K) (at %). (PM) primitive mantle (Sun, McDonough, 1989).
* Analyses from (Vetrin and Kalinkin, 1992).

**Table 6.** Normative composition (wt %) of xenoliths

| End member | 37-30 | E/96-10(3) | E/96-10(1) | E/96-10(2) | 16/89 | 37-40 | 37-3(4) | 37-60 | 67-12 | 37-52 | 37-2 | 37-9(4) | 41-5 |
|---|---|---|---|---|---|---|---|---|---|---|---|---|---|
| *Qtz* | | 6.4 | 0.6 | | | | | 1.6 | 3.7 | 3.3 | 2.3 | 8.5 | |
| *Ab* | 12.7 | 14.8 | 19.9 | 33.9 | 34.2 | 48.8 | 32.6 | 32.6 | 28.0 | 28.0 | 35.2 | 8.5 | 15.4 |
| *An* | 22.2 | 18.3 | 24.2 | 25.0 | 29.0 | 21.3 | 20.6 | 21.6 | 16.1 | 23.4 | 17.2 | 1.3 | 9.2 |
| *Or* | 2.9 | 3.7 | 5.1 | 7.5 | 7.8 | 6.0 | 5.2 | 14.3 | 6.8 | 7.1 | 12.3 | 2.0 | 1.0 |
| *Di* | 28.6 | 0.0 | 12.5 | 4.3 | 2.1 | 0.3 | 12.3 | 5.8 | 13.2 | 10.4 | 9.4 | | 55.6 |
| *Ol* | 11.1 | 0.0 | | 0.9 | | 6.2 | 2.5 | | | | | | 5.5 |
| *Opx* | 10.7 | 34.6 | 24.0 | 19.2 | 15.4 | 5.8 | 19.4 | 12.4 | 24.5 | 20.6 | 16.2 | 57.0 | |
| *Ne* | | | | | | | | | | | | | 3.9 |
| *Cal* | 2.1 | 5.2 | 4.8 | 3.7 | 4.1 | 4.3 | 2.7 | 5.5 | 1.8 | 1.8 | 2.3 | 6.3 | |
| *Ilm* | 2.2 | 2.1 | 1.6 | 1.4 | 2.1 | 1.3 | 1.3 | 1.2 | 2.5 | 1.4 | 1.8 | 0.8 | 2.4 |
| *Mag* | 7.6 | 6.7 | 5.7 | 3.3 | 4.7 | 5.0 | 3.1 | 4.7 | 2.3 | 3.8 | 2.2 | 10.5 | 6.5 |
| *Als* | | 6.8 | | | | | | | | | | 3.9 | |
| *Ap* | | 0.8 | 1.5 | 0.7 | 0.4 | 0.9 | 0.2 | 0.2 | 1.0 | | 1.0 | 0.2 | 0.4 |
| *Fl* | | 0.5 | 0.1 | 0.1 | 0.1 | 0.1 | 0.1 | 0.1 | 0.2 | 0.1 | 0.1 | 1.0 | 0.1 |
| *An*/(*Ab* + *An*) | 0.62 | 0.55 | 0.55 | 0.42 | 0.46 | 0.30 | 0.39 | 0.40 | 0.43 | 0.46 | 0.33 | 0.13 | 0.37 |

Note: *Als*—alsilite ($Al_2SiO_5$), *Ne*—nepheline, *Fl*—fluorite, *Ilm*—ilmenite, other mineral symbols as in Tables 1 and 2.

**Table 7.** Sm–Nd isotopic data on ultrabasic lamprophyres and xenoliths

| no. | Sample | Rock | Supposed age, Ma | Sm, ppm | Nd, ppm | $^{147}Sm/^{144}Nd$ | $^{143}Nd/^{144}Nd$ | $\varepsilon_{Nd}(0)$ | $\varepsilon_{Nd}(T)$ | $T_{Nd}$(DM-1st) | $T_{Nd}$(DM-2st) |
|---|---|---|---|---|---|---|---|---|---|---|---|
| 1 | E/96-1(1) | UBL | 360 | 10.6 | 75.34 | 0.08505 | 0.512332 | −6.0 | −0.84 | 971 | – |
| 2 | E/96-20(1) | same | same | 7.05 | 45.38 | 0.09396 | 0.512116 | −10.1 | −5.57 | 1314 | – |
| 3 | 37-42-1* | ″ | ″ | 8.90 | 62.52 | 0.0868 | 0.512347 | −5.7 | −0.6 | 966 | |
| 4 | E/96-10(3) | Garnet granulite | 2450 | 3.45 | 12.23 | 0.15747 | 0.511902 | −14.4 | −2.04 | 3365 | 2621 |
| 5 | E/96-10(1) | same | same | 3.98 | 16.03 | 0.14772 | 0.51172 | −17.9 | −2.52 | 3286 | 2759 |
| 6 | E/96-10(2) | ″ | ″ | 2.8 | 12.98 | 0.13059 | 0.511623 | −19.8 | 1.00 | 2789 | 2644 |
| 7 | 37-20 | ″ | ″ | 3.36 | 16.57 | 0.12233 | 0.511357 | −10.7 | −1.60 | 2976 | 2940 |
| 8 | 16/89* | ″ | ″ | 4.771 | 22.09 | 0.1305 | 0.51168 | −18.7 | 2.15 | 2683 | 2551 |
| 9 | 37-40* | ″ | ″ | 5.566 | 30.9 | 0.1089 | 0.511316 | −24.8 | 1.86 | 2582 | 2710 |
| 10 | 37-3(4)* | ″ | ″ | 3.004 | 13.81 | 0.1315 | 0.511546 | −21.3 | −0.79 | 2960 | 2782 |
| 11 | 37-2 | ″ | ″ | 6.68 | 40.13 | 0.1006 | 0.511194 | −28.2 | 2.10 | 2625 | 2858 |
| 12 | 41-5 | Garnet pyroxenite | ″ | 9.85 | 51.91 | 0.11466 | 0.511414 | −23.9 | 1.95 | 2661 | 2727 |

Note: The measurements were conducted on a Finnigan MAT-262 mass spectrometer (analyst A.A. Delenitsin, Geological Institute, Kola Science Center, Russian Academy of Sciences). $^{143}Nd/^{144}Nd$ values of standards: 0.511833 ± 6 ($n$ = 11) for LaJolla and 0.512078 ± 5 ($n$ = 10) for JiNd1. The calculations according to the single stage [T(DM-1st)] and two-stage [T(DM-2 st)] models were conducted following the model in (Liew and Hofmann, 1988). UBL—ultrabasic lamprophyre. * Data from (Neymark et al., 1993).

amphibolization, and phlogopitization have not significantly modified the original composition of the protoliths of the xenoliths.

Granulite-facies metamorphism of the basic rocks is believed to have been nearly isochemical in terms of major and most incompatible and ore elements (REE, Y, Zr, Nb, Ti, Cr, Co, Ni, V, and others), which enabled us to utilize these elements to calculate the composition of the protoliths (Predovskii, 1980; Kremenetskii and Ovchinnikov, 1986; Afanas'ev et al., 2001). Conversely, the contact influence of the ultrabasic lamprophyres on the xenoliths resulted in the enrichment of the

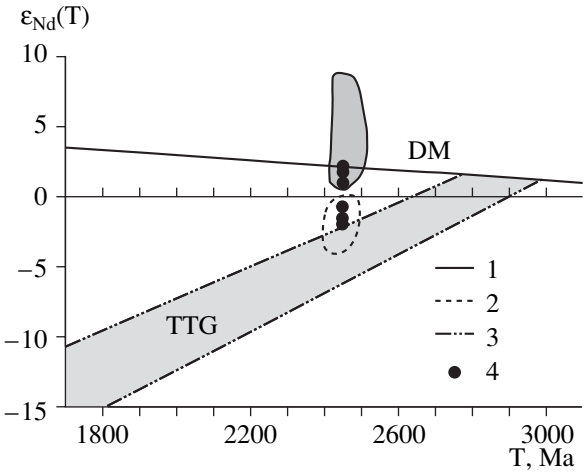


**Fig. 8.** Diagram $\varepsilon_{Nd}$–T. DM is the Nd evolution in the depleted mantle (Goldstein and Jacobsen, 1988).

Fields of the evolution of Nd isotopic composition: (1) basic–ultrabasic volcanic rocks of Archean greenstone belts in the Kola Peninsula (Vetrin et al., 2003; Vrevskii et al., 2003) and northern Karelia (Mil'kevich et al., 2003); (2) compositional field of Early Proterozoic layered intrusions; (3) tonalite–trondhjemite granitoids of Archean granite–greenstone terrane in the Kola Peninsula (Timmerman and Daly, 1995; Vetrin et al., 2003); (4) data points of xenoliths.

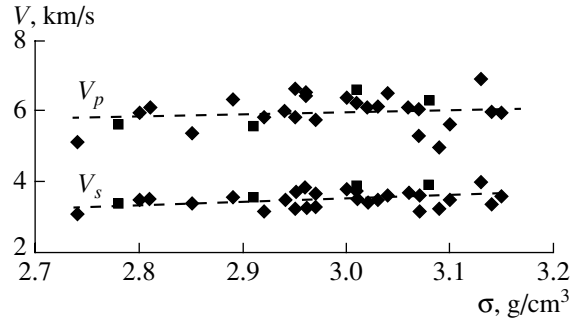


**Fig. 9.** Correlations between $V_p$ and σ and $V_s$ and σ for garnet granulites (diamonds) and pyroxenites (squares). Dashed lines are regression lines.

latter in CaO, MgO, and $CO_2$ (adding up to 5–6 wt %) and in some trace elements (Nb, Ba, Sr, and P). Since the concentrations of all major oxides in the analyses are normalized to 100 wt %, the effect of carbonatization of the xenoliths can be inferred from a decrease in the concentrations of other major components and, correspondingly, changes in the original contents and proportions of major oxides in the xenoliths. Because of this, the xenoliths can be compared with their possible volcanic analogues at the surface mainly using their normative composition in a *Ol* (norm)– *Qtz* (norm)–mg# diagram and the concentrations of incompatible elements (except Nb, Ba, Sr, and P) whose contents were the least susceptible to the carbonatization of rocks.

Our results presented above on the Sm–Nd systems and the age of zircons from the xenoliths indicate that these rocks were likely produced by the contamination of the Proterozoic protoliths with Archean material of basic composition. Inasmuch as the proportions of Archean and Proterozoic material in the xenoliths have not been evaluated and could likely vary within broad limits, we compared the xenoliths with basic and basic–intermediate rocks of various age in subvolcanic structures and massifs in the Kola Peninsula and northern Karelia: Proterozoic complexes of magmatic rocks (Belomorian coronites, gabbro-anorthosite massifs, layered intrusions of peridotite–pyroxenite–gabbronorite composition and their comagmatic volcanics) and with metamorphosed volcanic rocks of the Late

**Table 8.** Density (σ) and the velocities of longitudinal ($V_p$) and transverse ($V_s$) seismic waves in the xenoliths and their $V_p/V_s$ ratios

| Rock | σ, g/cm³ | | $V_p$, km/s | |
|---|---|---|---|---|
| | **1** | **2** | **1** | **2** |
| Garnet granulites | 2.7–3.15 (39) | 2.97 ± 0.11 | 5.02–6.98 (28) | 6.03 ± 0.47 |
| Pyroxenites | 2.78–3.13 (8) | 2.87 ± 0.26 | 5.58–6.64 (4) | 6.04 ± 0.53 |
| Whole selection | 2.7–3.15 (47) | 2.96 ± 0.11 | 5.02–6.98 (32) | 6.03 ± 0.47 |
| Rock | $V_s$, km/s | | $V_p/V_s$ | |
| | **1** | **2** | **1** | **2** |
| Garnet granulites | 3.19–4.01 (27) | 3.52 ± 0.23 | 1.54–1.96 (27) | 1.72 ± 0.09 |
| Pyroxenites | 3.39–3.93 (4) | 3.69 ± 0.23 | 1.57–1.71 (4) | 1.64 ± 0.06 |
| Whole selection | 3.19–4.01 (31) | 3.54 ± 0.26 | 1.54–1.96 (31) | 1.71 ± 0.09 |

Note: The measurements were conducted at the laboratory of Geophysics, Geological Institute, Kola Research Center, Russian Academy of Sciences. (**1**) Range of values (numerals in parentheses correspond to the numbers of samples); (**2**) average values and standard deviations.

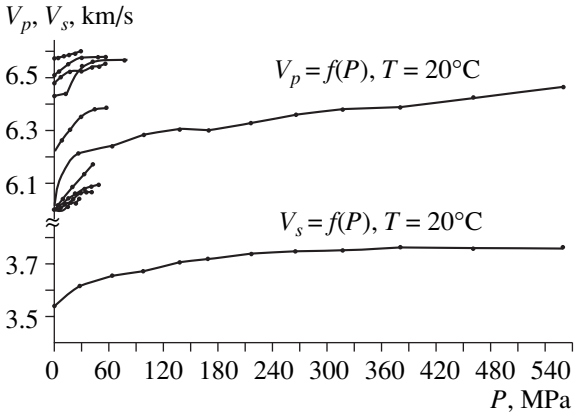


**Fig. 10.** $V_p$, $V_s$–$P$ diagram for garnet granulite xenoliths.

Archean greenstone belts. The results of approximately 300 recalculated rock analyses are presented in Fig. 11.

**Coronite (lherzolite–gabbronorite) intrusions** occur predominantly in the Belomorian Mobile Belt, where they compose lens- and dike-shaped bodies and massifs up to 80 km$^2$ (Stepanov, 1981; Sharkov et al., 2004). The age of the coronites (drusites) is 2.40–2.45 Ga, and their $\varepsilon_{Nd}$ values range from –1.9 to +0.2, with the strong predominance of negative values (Lobach-Zhuchenko et al., 1998). The coronites are dominated by gabbronorites and also include plagioclase lherzolites, anorthosites, and gabbro-diorites of the Mg- and Fe-series (Stepanov, 1981; Lobach-Zhuchenko et al., 1998). Most of the coronites affiliate with the Mg-series, whose rocks compose both individual massifs and parts of composite massifs.

**Layered intrusions** of the peridotite–pyroxenite–gabbronorite association in the central part of the Kola Peninsula compose an extended belt, which is spatially restricted to the northern and northwestern surroundings of the Imandra–Varzuga paleoriftogenic belt. The intrusions include differentiated ultrabasic–basic bodies (Moncha pluton and the massifs of the Pana Tundra and Fedorova Tundra) and norite–gabbronorite massifs of the Imandra Complex. The U–Pb and Sm–Nd ages of the Pana Tundra Massif are 2501–2491 and 2487 ± 51 Ma, respectively, $\varepsilon_{Nd}$ = –2.1 ± 0.5 (Amelin et al., 1995; Chistyakova et al., 2000; Balashov et al., 1993). The U–Pb age of the Imandra Complex is 2441–2434 Ma, and its Sm–Nd age is equal to 2444 ± 77 Ma, $\varepsilon_{Nd}$ = –2.0 ± 0.6 (Balashov et al., 1993; Amelin et al., 1995). The age of the complex is close to the age of the volcanic rocks of the Seidorechka suite (2448 ± 8 Ma; Bayanova and Chashchin, 2001) in the Paleoproterozoic Imandra–Varzuga structure. Along with compositional similarities, this suggests the comagmatic character of these rocks (Melezhik and Sturt, 1994; Smol'kin et al., 2004). The composition of the Imandra rocks, their age, and accompanying ore mineralization are similar to those of the coronites and younger (2445–2435 Ma) layered intrusions localized mostly in Karelia and Finland (the Burakovskaya intrusion and the Koitelainen, Ankavaara, and other massifs). This group of intrusions is close in age to gabbro–anorthosite massifs in western Belomorie (Stepanov, 1981). The largest of them in the southern Kola Peninsula is the Kolvitsa Massif, which is dominated by gabbro–anorthosites, anorthosites, and norites. Magmatic zircon from the anorthosites of the Kolvitsa Massif was dated at 2450 ± 10 Ma (Mitrofanov et al., 1993) and 2462 +7/–6 Ma (Frish et al., 1995).

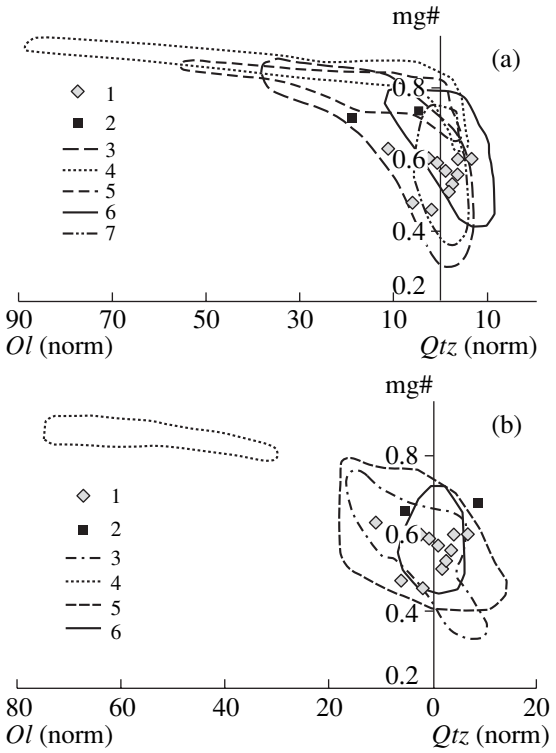


**Fig. 11.** *Ol*(norm)–*Qtz*(norm)–mg# diagrams for the composition of (a) Proterozoic and (b) Archean complexes.

(a) (1) Garnet granulites; (2) pyroxenites; (3) coronites (Stepanov, 1981; Lobach-Zhuchenko et al., 1998); (4, 5) layered intrusions: (4) Monchegorsk district (*Imandra–Varzuga…*, 1982); (5) massifs of the Fedorova–Pana Tundras (*Imandra–Varzuga…*, 1982; Melezhik and Sturt, 1994); (6) rocks of the Imandra complex and metamorphosed volcanic rocks of the Seidorechka suite (Mitrofanov et al., 1995; Melezhik and Sturt, 1994; Mints et al., 1996); (7) gabbro-anorthosites of the Kola Peninsula (Mints et al., 1996; Terekhov and Levitskii, 1993) and Karelia (Stepanov, 1981).

(b) (1) Garnet granulites; (2) pyroxenites; (3) metamorphosed volcanic rocks of the Kolmozero–Voronja greenstone belt (Mints et al., 1996); (4) komatiites of the Kola Peninsula (Vrevskii et al., 2003); (5, 6) metamorphosed volcanic rocks of greenstone belts: (5) Terskii–Notozero (*Volcanism…*, 1987; Kremenetskii, 1979; Vetrin et al., 2003), (6) Tikshozero (Mil'kevich et al., 2003).

The results of our research demonstrate that the coronites are compositionally more diverse, with mg# varying from 0.27 to 0.89 and with the predominance of olivine-normative rocks over quartz-normative variet-

ies (Fig. 11a). According to these parameters, the xenoliths plot between the coronites of the Mg- and Fe-series in the *Ol*(norm)–*Qtz*(norm)–mg# diagram. Their trace-element composition is most closely approximated by those of the coronites of the Fe-series, and these rocks differ from the Mg-series coronites in having higher concentrations of most incompatible elements (Fig. 12a). The exception is Rb, whose lower concentrations in the xenoliths are most probably explained by the migration of this element in synmetamorphic fluids, which were produced by the dehydration of rocks under granulite facies conditions (Moorbath and Taylor, 1986). The compositional similarities between the lower crustal xenoliths and the Fe-series coronites were also emphasized by other researchers (Kempton et al., 2001).

**The rocks of ancient layered intrusions** (massifs in the Monchegorsk district and the Fedorova–Pana intrusion) are more magnesian than the xenoliths (mg# = 0.70–85 and 0.46–0.68, respectively) and are mostly undersaturated in silica (are olivine-normative). Because of this, most of the data points of the layered intrusions plot in the left-hand side of the *Ol*(norm)–*Qtz*(norm)–mg# diagram (Fig. 11a), away from the compositional field of the xenoliths. The rocks are characterized by much lower REE and Ti concentrations than those of the xenoliths (Fig. 12a).

In contrast to the ancient layered intrusions, the norites and gabbronorites of the Imandra Complex are dominated by quartz-normative rocks with mg# = 0.68–0.78, which plot in the *Ol*(norm)–*Qtz*(norm)–mg# diagram within the continuation of the compositional field of the Seidorechka suite rocks, a fact confirming the comagmatic character of these rocks (Melezhik and Sturt, 1994; Smol'kin et al., 2004). The compositional field of the metamorphosed volcanic rocks of the Seidorechka suite is, in turn, significantly overlapped by the compositional field of the lower crustal xenoliths (Fig. 11a). Compositional similarities between low-Ti basalts and basaltic andesites of the Seidorechka suite and the lower crustal xenoliths also follow from the identity of their REE, Zr, and Ti patterns (Fig. 12a). The trace-element composition of the xenoliths is close to those not only of the metamorphosed volcanics of the Seidorechka suite but also of the rocks of the Il'mozero and Umba suites (Fig. 12b), which compose the middle part of the volcanogenic stratigraphic sequence of the Imandra–Varzuga structure.

The gabbro–anorthosite massifs in Karelia and the Kolvitsa Massif are dominated by quartz-normative rocks with mg# = 0.4–0.7, and the compositional field of these rocks overlaps the fields of the metavolcanics of the Seidorechka suite and the lower crustal xenoliths (Fig. 11a). This led as to regard the gabbro-anorthosites as rocks close in composition to the lower crustal xenoliths (Vetrin and Kalinkin, 1992). At the same time, the xenoliths differ from the rocks of these complexes by the absence of typical anorthosites with high alumina contents (up to 25–30 wt % $Al_2O_3$).

**The Late Archean greenstone belts** include the Kolmozero–Voronja belt (Northern Kola; Smol'kin et al., 2000) and the Terskii–Notozero belt in the Kola geoblock and the Tikshozero belt in the northern part of the Belomorian terrane. The greenstone belts are characterized by the abundance of komatiites, basalts, and basaltic andesites in the lower portion of the stratigraphic sequence, whereas its upper parts consist of terrigenous complexes and acid volcanics. Volcanism occurred in the greenstone belts of the Kola Peninsula and northern Karelia at 2.8–2.9 Ga (Vrevskii et al., 2003). The rocks of the western and eastern parts of the Terskii–Notozero belt are thought to have served as the basement for the Paleoproterozoic Pechenga–Imandra–Varzuga structure (Dobrzhinetskaya et al., 1995). Granitization processes and later deformations resulted in the ubiquitous fragmentation of the rocks composing this structure, which are now preserved merely as relict domains among volumetrically predominant granitoids of the granite–greenstone terranes.

The data points of the volcanics of the Kolmozero–Voronja, Terskii–Notozero, and Tikshozero greenstone belts define elongated trends from komatiites to quartz tholeiites, basaltic andesites, and andesites in the *Ol*(norm)–*Qtz*(norm)–mg# diagram. The range of mg# = 0.5–0.7 is characterized by the partial overlap of the fields of the xenoliths and metavolcanics, with most of the xenoliths corresponding to metatholeiites (Mil'kevich et al., 2003) or komatiite basalts with MgO contents from 8 to >10 wt % (Mints et al., 1996). Most of these rocks contain 0.5–5.0% normative quartz, with more rare silica-undersaturated varieties bearing 2–13% normative olivine. The trace-elements patterns of the rocks normalized to the primitive mantle clearly demonstrate the differences between rocks from discrete greenstone belts (Fig. 12c). The lowest Rb and LREE concentrations are typical of the rocks from the Kolmozero–Voronja greenstone belt, which is consistent with data on the origin of these rocks from a mantle source depleted in trace elements (*Greenstone Belts*..., 1988; Vrevskii et al., 2003). Elevated concentrations of these elements were detected in the metabasalts of the Terskii–Notozero belt, and the highest concentrations of these elements, close to those in TH2 basalts (Condie, 1981), were found in the rocks of the Tikshozero greenstone belt. Simultaneously the $(La/Yb)_n$ ratio increases and is equal to 1.5, 2.4, and 3.8, respectively. The trace-element composition of the lower crustal xenoliths is the most similar to that of the metatholeiites of the Tikshozero greenstone belt, except only lower concentrations of La and Ce and slightly elevated concentrations of HREE and Y in the latter.

The results of our comparative analysis demonstrate that the major- and trace-element compositions of the xenoliths are similar to those of both the magmatic rocks of Paleoproterozoic age and the volcanics of Late

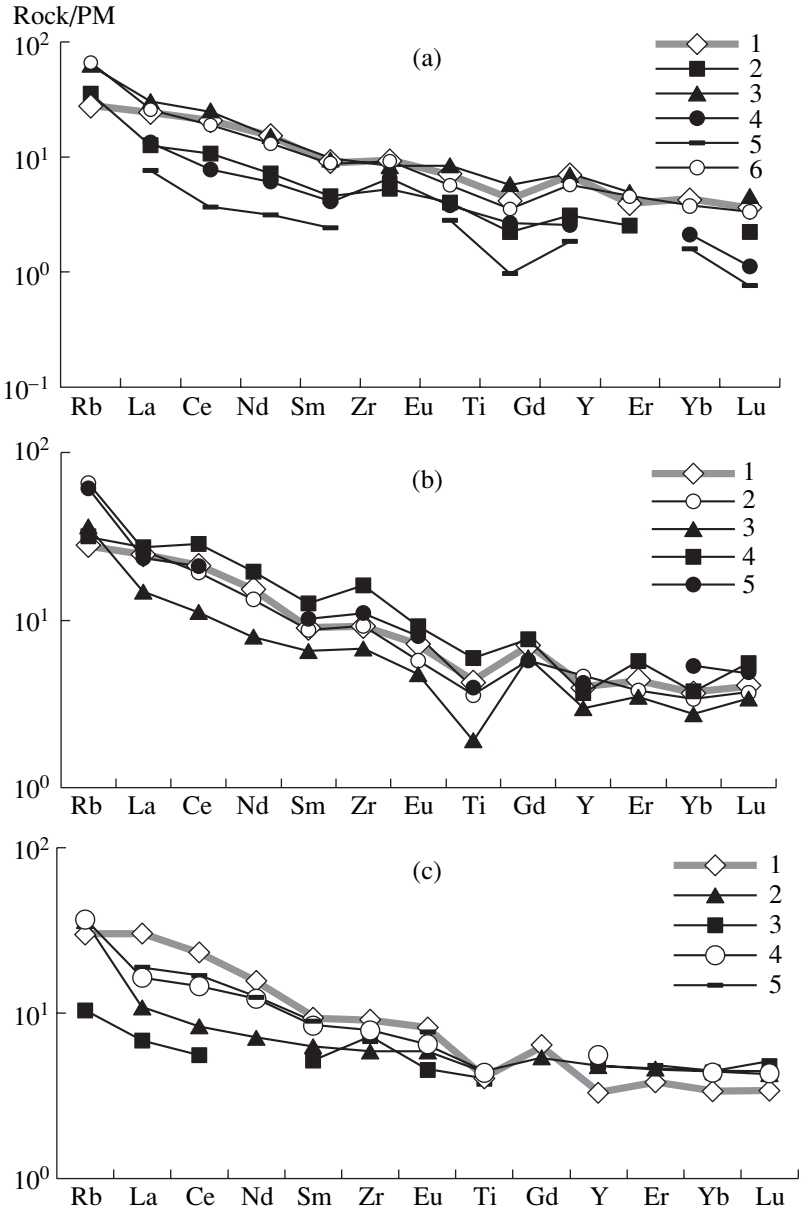


**Fig. 12.** Primitive mantle-normalized (Sun and McDonough, 1989) trace-element patterns for (a) rocks of Proterozoic complexes, (b) metamorphosed volcanics of the Imandra–Varzuga structure, and (c) Archean rocks.

(a) (1) Xenoliths; (2, 3) coronites (Lobach-Zhuchenko et al., 1998): (2) Mg-coronites, (3) Fe-coronites; (4) Imandra Complex (Melezhik and Sturt, 1994); (5) massifs of the Fedorova–Pana Tundras (Melezhik and Sturt, 1994); (6) metamorphosed volcanic rocks of the Seidorechka suite (Melezhik and Sturt, 1994).

(b) (1) Xenoliths; (2–5) metamorphosed volcanic rocks of the of the Imandra–Varzuga structure (Melezhik and Sturt, 1994): (2) Seidorechka suite, (3) Polisarskaya Formation, (4) Umba Formation, (5) Il'mozero suite.

(c) (1) Xenoliths; (2–4) metamorphosed volcanic rocks of greenstone belts; (2) Terskii–Notozero (Vetrin et al., 2003), (3) Kolmozero–Voronja (Mints et al., 1996), (4) Tikshozero (Mil'kevich et al., 2003), (5) Archean amphibolites TH2 (Condie, 1981).

Archean greenstone belts. Among the Paleoproterozoic magmatic rocks, the xenoliths resemble most closely the rocks of younger layered intrusions of the Imandra norite–gabbronorite complex, their comagmatic volcanics, coronites, and the rocks of the gabbro–anorthosite complex, and, among the Late Archean volcanic rocks, metatholeiites of the Tikshozero greenstone belt.

### *Stages of Lower Crustal Growth*

The lower crust in the Belomorian Mobile Belt (BMB) was generated in close relation to the development of this belt as a collision zone between the Kola and Karelia cratons. The evolutionary history of this structure includes the Late Archean accretionary–collisional and Early Proterozoic rifting stages (Volodichev,

1990; *Geology…*, 1995; Glebovitskii, 1993). The predominant upper crustal magmatic rocks of the Late Archean stage are granitoids dated at 2.75–2.65 Ga (Lobach-Zhuchenko et al., 1998) and less widely spread rocks of the tholeiitic and calc–alkaline series of the northern Karelian system of greenstone belts (2.88–2.82 Ga; Bibikova et al., 1999). Data on the age and composition of the lower crust of this stage are still scarce and are limited to zircon dates for lower crustal xenoliths (Vetrin, 1998; Downes et al., 2002) and materials demonstrating similarities between the major- and trace-element compositions of these xenoliths and the volcanics of Late Archean greenstone belts. These data and materials provide reasons to believe that the BMB was underlain by a mafic lower crust already in the Late Archean, with this crust roughly corresponding to the tholeiitic volcanics of the Tikshozero greenstone belt.

In the Early Paleoproterozoic (2.6–2.2 Ga), the BMB was characterized by the development of nappe–folded structures dipping toward the Kola craton. The same time was responsible for the origin of numerous coronite bodies, which were affected (together with their host gneisses) by intense tectono-metamorphic reworking under amphibolite-facies conditions. The Lapland–Umba granulite belt, to which gabbro–anorthosite massifs are spatially restricted, was formed in the northern part of the belt. Simultaneously, the Pechenga and Imandra–Varzuga rift structures developed in the Kola craton, and layered peridotite–pyroxenite–gabbronorite and norite–gabbronorite intrusions were emplaced into the surroundings of latter structure. Some of these intrusions are comagmatic with the Sumian–Sariolian volcanic rocks in the Imandra–Varzuga structure.

The origin of gabbro–anorthosite and coronite bodies, layered intrusions, and volcanic rocks in the upper crust was associated with underplating: the emplacement of melts compositionally close to the upper crustal rocks into the Late Archean mafic lower crust. These melts underwent crystallization differentiation, which likely took place under olivine control, as follows from the direct correlation between the mg# of the xenoliths and their Ni concentrations (Fig. 6b). The intense tectonic recycling of the upper portions of the BMB crust during this period of time induced the plastic flow of the lower crustal material and the development of banded and taxitic textures in the garnet granulites. The plastic deformations were facilitated by the likely long-lasting preservation of residual melts in the cumulates, which enabled the motions of both tabular basic intrusions and overlying Neoarchean rocks.

It is thus reasonable to hypothesize that the Early Paleoproterozoic stage of lower crustal growth in the BMB took place at the strong heating of the material because of the emplacement of abundant mantle melts into the mafic Neoarchean crust and the induced plastic flow of the material and its homogenization under granulite-facies conditions.

In the Late Paleoproterozoic (2.2–1.7 Ga), the most widespread processes transforming the lower crust involved its phlogopitization (2.1–2.0 Ga; Kempton et al., 2001) and migmatization (1.9–1.7 Ga; Vetrin and Nemchin, 1998). The migmatization of the lower crust was coeval with the development of mica pegmatites and the emplacement of intrusions of granite porphyries (Savitskii et al., 1998; Vetrin et al., 2002), whereas the phlogopitization of the garnet granulites could be caused by the resumption of magmatic activity in the Imandra–Varzuga structure. The latest manifestations of magmatic activity in the lower crust involved the processes of alkaline metasomatism and amphibolization at 0.43–0.39 Ga (Beard et al., 1996; Arzamastsev and Belyatskii, 1999; Vetrin and Travin, 2003), which predated the emplacement of the ultrabasic melts of the diatremes and dikes with lower crustal xenoliths.

### *Protoliths of the Garnet Granulites*

Available data suggest that the thickening of the Late Archean lower crust in Early Paleoproterozoic was achieved by the emplacement of melts, which formed a Paleoproterozoic province of 2.4- to 2.5-Ga magmatic rocks in the upper crust (Sharkov et al., 1999; Kempton et al., 2001). Since the Sm–Nd isotopic systems of the xenoliths were not significantly perturbed under the effect of the ultrabasic lamprophyre melts, we were able to evaluate the contributions of the Archean and Proterozoic material to the lower crustal xenoliths by the model of two-component mixing (Jahn et al., 2000)

$$X^m = (\varepsilon^c - \varepsilon^r)Nd_c/[(Nd_m - Nd_c) - (\varepsilon^m Nd_m - \varepsilon^c Nd_c)],$$

where $X^m$ is the content of the mantle component (%); $\varepsilon^c$, $\varepsilon^r$, and $\varepsilon^m$ are the Nd isotopic compositions of, respectively, the crustal, modified in the rock, and mantle components; and $Nd_c$ and $Nd_m$ are the Nd concentrations in the crustal and mantle components. The mantle component consisted of the Early Proterozoic norites–gabbronorites of the Imandra Complex (T = 2444 ± 77 Ma, $\varepsilon_{Nd} = -2 \pm 0.6$, Nd = 10.9 ppm; Balashov et al., 1993), and the crustal component was made up of basaltoids of the Late Archean Tikshozero greenstone belt (T = 2820 ± 130 Ma, $\varepsilon_{Nd}$ = 3.4 ± 0.4, Nd = 12.5 ppm; Mil'kevich et al., 1993).

Calculations indicate that the percentage of the mantle component in the xenoliths varies from 8 to 99%, and all of our samples plot within two discrete fields: with high (68–99%) and relatively low (8–33%, Fig. 13a) $X^m$ values. In compliance with the assumed model, the samples with low $X^m$ values can be regarded as metamagmatic rocks of Archean age that were variably affected by Paleoproterozoic melts, whereas samples with high contents of the mantle component were likely derivatives of Paleoproterozoic melts relatively weakly contaminated with the material of the Archean protocrust. The two groups are separated by a compositional gap with roughly equal contents (~30%) of the crustal material in the Paleoproterozoic melts and the

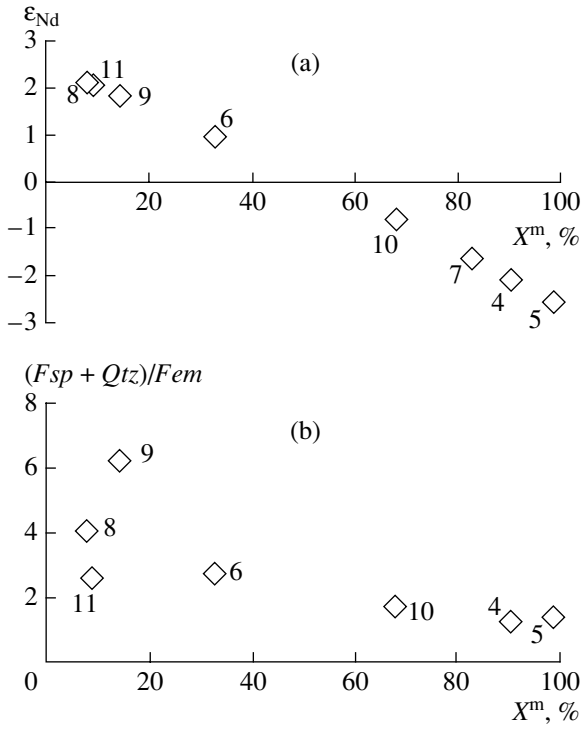


**Fig. 13.** Correlations of the mantle component contents ($X^m$) with (a) $\varepsilon_{Nd}$ and (b) (*Fsp* + *Qtz*)/*Fem*, where *Fem* is the sum of the contents of pyroxene and garnet. Numerals in the diagrams correspond to analysis numbers in Table 7.

latter in the rocks of the Archean protocrust. The correlation between $X^m$ and the (*Fsp* + *Qtz*)/*Fem* ratio (Fig. 13b) is explained by the lower mg# values and higher contents of normative quartz in the metavolcanics of the Tikshozero greenstone belt than those of the gabbro and gabbronorites of the Imandra Complex.

### *Compositional and Structural Heterogeneity of the Lower Crust*

The heterogeneous structure of the lower crust of BMB, which was inferred from the results obtained on the deep xenoliths, is in general agreement with the data of deep seismic sounding of the territory (Sharov, 1993; Tripol'skii and Sharov, 2004). According to these data, the most clearly pronounced lithospheric boundary is the Moho discontinuity (M), whose position determines the crustal thickness in the central and southern parts of the Kola Peninsula (40–44 km). The velocities of longitudinal seismic waves at M are 8.0–8.2 km/s and increase to 8.5–8.7 km/s at a depth of 200 km. The predominant upper mantle rocks at this depth are ultrabasic spinel and garnet peridotites.

The inner structure of the Earth's crust is assumed to be described by a three-layer model with a complex mosaic–block architecture, which reflects the multistage character of the tectono-magmatic metamorphic reworking of the crust. The lower crust (the basaltic or granulite–basite layer) beneath the Kola Peninsula has a thickness from 10 to >20 km and is believed to consist of basic rocks. The highest thickness of the lower crust was determined in the boundary zones between large crustal blocks, including the Belomorian Mobile Belt between the Karelian and Kola cratons.

As was demonstrated above, the experimentally determined velocities of seismic waves $V_p$ and $V_s$ in the xenoliths are much lower than the values determined by the seismic sounding of the lower crust beneath the Baltic Shield. These discrepancies between the velocities of seismic waves suggest that the regional lower crust is heterogeneous, and the granulites contain intercalations and lenses of denser rocks of ultrabasic composition, which are characterized by higher velocities. These rocks can likely be spinel peridotites, whose xenoliths were brought to upper crustal levels together with xenoliths of garnet granulites and pyroxenites (Vetrin and Kalinkin, 1992). Assuming the average $V_p$ and $V_s$ values in upper-mantle ultrabasic rocks equal to 8.18 and 4.68 km/s, respectively (Rudnik and Fountain, 1995), and the analogous values for the lower crustal rocks of the Baltic Shield to be, respectively, 7.23 and 4.13 km/s (Grad and Luosto, 1987), the overall amount of ultrabasic rocks in the regional lower crust can be evaluated at 8–10%. Inasmuch as the results of deep seismic sounding (Tripol'skii and Sharov, 2004) point to an increase in the wave velocities from $V_p$ = 6.5–6.8 km/s at upper crustal levels to 6.9–7.3 and 7.4–7.5 km/s at intermediate and lower levels (near M), respectively, it is logical to conclude that the content of ultrabasic rocks increases from the upper to lower levels of the crust. Provided that the composition of the lower crust has not changed since the emplacement of the Devonian dikes and diatremes, the data obtained on the composition and physical characteristics of the xenoliths testify to the occurrence of a crustal–mantle layer at the boundary between the crust and upper mantle.

## CONCLUSIONS

The lower crust of the Belomorian Mobile Belt is dominated by garnet granulites and pyroxenites, which occur in the form of xenoliths in Devonian diatremes and dikes in the southern part of the Kola Peninsula. When entrained to the surface by ultrabasic melts, the xenoliths were recycled by fluids and enriched in CaO, MgO, and some trace elements, such as Ba, Nb, Sr, and P. The concentrations of some trace elements (Sm, Nd, Y, Ti, Zr, Ni, Cr, and others) and the Sm–Nd isotopic composition of the xenoliths were not significantly modified, and this enabled us to use these elements to compare the xenoliths with regional subvolcanic complexes and to calculate the composition of the protoliths.

The evolutionary history of the BMB was subdivided into two major stages: Neoarchean and Early Paleoproterozoic. The origin of the mafic lower crust in the Late Archean was related to the emplacement of

significant volumes of basic melts into the lowermost crustal levels. Analogues of these melts in the upper lithosphere are the initial volcanics of the Northern Karelian system of greenstone belts. The further growth of the Late Archean crust in the Early Paleoproterozoic proceeded during the emplacement of melts that gave rise to layered intrusions at upper crustal levels and their comagmatic volcanic rocks and intrusions of coronites and gabbro-anorthosites. The results obtained on the Sm–Nd systematics of the xenoliths indicate that the percentage of Paleoproterozoic material ($X^m$) in them varied from 8 to 99%. Proceeding from the assumed model of two-component mixing (Jahn et al., 2000), the samples with low $X^m$ values can be interpreted as Archean magmatic rocks variably affected by the Paleoproterozoic melts, whereas the samples with high $X^m$ values were likely derivatives of the Paleoproterozoic melts relatively weakly contaminated with the material of the Archean protocrust. The emplacement of significant volumes of melts into the lower crust induced its heating and transition into a state susceptible to viscous–plastic flow, which facilitated the origin of rocks with variable proportions of the Late Archean and Early Proterozoic material. The process of the viscous–plastic flow of the rocks likely also affected the upper mantle, as follows from the occurrence of foreign rock fragments among the garnet granulites, with the amount of mantle xenoliths increasing from the top to bottom of the lower crust.

The further transformations of the lower crustal rocks in the Late Paleoproterozoic (origin of phlogopite and granitization) occurred locally and did not significantly modify the composition of the lower crust. The youngest manifestations of endogenic activity were the Paleozoic processes of alkaline metasomatism and amphibolization, which predated the emplacement of the Devonian diatremes and dikes with xenoliths.

## ACKNOWLEDGMENTS

The authors thank participants of the EUROPROBE SVEKALAPKO Project, H. Downes, A. Beard (Birkbeck College, University of London, London, United Kingdom), and Yu.A. Balashova (Geological Institute, Kola Science Center, Russian Academy of Sciences) for valuable discussion of the problems formulated in the manuscript. We appreciate constructive comments expressed by E.V. Sharkov and A.V. Girnis (Institute of the Geology of Ore Deposits, Petrography, Mineralogy, and Geochemistry, Russian Academy of Sciences), which were taken into account during the preparations of the final version of the manuscript. This study was financially supported by the Russian Foundation for Basic Research (project nos. 02-05-64394 and 03-05-64169).

## REFERENCES

1. M. A. Afanas'eva, N. Yu. Bardina, O. A. Bogatikov, et al., *Petrography and Petrology of the Magmatic, Metamorphic, and Metasomatic Rocks* (Logos, Moscow, 2001) [in Russian].
2. Y. V. Amelin, L. M. Heaman, and V. S. Semenov, "U–Pb Geochronology of Layered Mafic Intrusions in the Eastern Baltic Shield: Implications for the Timing and Duration of Paleoproterozoic Continental Rifting," Precambrian Res. **75**, 31–46 (1995).
3. A. A. Arzamastsev and B. V. Belyatskii, "Evolution of the Mantle Source of the Khibiny Massif: Evidence from Rb–Sr and Sm–Nd Data on Deep-Seated Xenoliths," Dokl. Akad. Nauk **366** (3), 387–391 (1999) [Dokl. Earth Sci. **366** (4), 562 (1999)].
4. A. A. Arzamastsev, B. V. Belyatsky, and L. V. Arzamastseva, "Agpaitic Magmatism in the Northeastern Baltic Shield: a Study of the Niva Intrusion, Kola Peninsula, Russia," Lithos **51**, 27–46 (2000).
5. V. V. Balaganskii, V. N. Glaznev, and L. G. Osipenko, "The Early Proterozoic Evolution of the Northeastern Baltic Shield: A Terrane Analysis," Geotektonika, No. 2, 16–28 (1998) [Geotectonics **32** (2), 81 (1998)].
6. Y. Balashov, T. Bayanova, and F. Mitrofanov, "Isotope Data on the Age and Genesis of Layered Basic–Ultrabasic Intrusions in the Kola Peninsula and Northern Karelia, Northeastern Baltic Shield," Precambrian Res. **64**, 197–205 (1993).
7. T. B. Bayanova and V. V. Chashchin, "New Results of Radiological Dating of the Acid Metavolcanic Rocks of the Kislaya Guba and Seiodorechka Formations," in *Proceedings of the 1st All-Russia Paleovolcanological Symposium, Petrozavodsk, Russia, 2001* (Petrozavodsk, 2001), pp. 16–17 [in Russian].
8. A. D. Beard, H. Downes, E. Hegner, et al., "Mineralogy and Geochemistry of Devonian Ultramafic Minor Intrusions of the Southern Kola Peninsula, Russia: Implications for the Petrogenesis of Kimberlites and Melilitites," Contrib. Mineral. Petrol. **130**, 288–303 (1998).
9. A. D. Beard, H. Downes, V. Vetrin, et al., "Petrogenesis of Devonian Lamprophyre and Carbonatite Minor Intrusions, Kandalaksha Gulf (Kola Peninsula, Russia)," Lithos **39**, 93–119 (1996).
10. E. V. Bibikova, A. I. Slabunov, S. V. Bogdanova, et al., "Early Magmatism of the Belomorian Mobile Belt, Baltic Shield: Lateral Zoning and Isotopic Age," Petrologiya **7** (2), 115–140 (1999) [Petrology **7** (2), 123 (1999)].
11. I. N. Bindeman, E. V. Sharkov, and D. A. Ionov, "Xenoliths of Biotite–Garnet–Orthopyroxene Rocks in the Dike-like Explosion Pipe of Elovy Island, White Sea," Zap. Vseross. Mineral. O-va **119** (3), 1–11 (1990).
12. W. V. Boynton, "Cosmochemistry of the Rare Earth Elements: Meteorite Studies," in *Rare Earth Element Geochemistry*, Ed. by P. Henderson (Elsevier, Amsterdam, 1984), pp. 63–114.
13. S. Yu. Chistyakova, T. B. Bayanova, O. V. Gogol, and A. A. Delenitsin, "Variations in the $^{87}Sr/^{86}Sr$ Ratios Across the Magnetite Gabbro Body in the Western Pana Tundra Layered Intrusion, Kola Peninsula," in *Proceedings of 2nd All-Russia Petrographic Conference, Syktyvkar, Russia, 2000* (Syktyvkar, 2000), Vol. 4, pp. 353–355 [in Russian].

14. S. Claesson, V. Vetrin, T. Bayanova, and H. Downes, "U–Pb Zircon Ages from a Devonian Carbonatite Dyke, Kola Peninsula, Russia: a Record of Geological Evolution from the Archaean to the Palaeozoic," Lithos **51**, 95–108 (2000).
15. L. F. Dobrzhinetskaya, O. Nordgulen, V. R. Vetrin, et al., "Correlation of the Archaean Rocks between the Sørvaranger Area, Norway, and the Kola Peninsula, Russia (Baltic Shield)," Geol. Unders. Spec. Publ. **7**, 7–28 (1995).
16. H. Downes, "The Nature of the Lower Continental Crust of Europe: Petrological and Geochemical Evidence from Xenoliths," Physics Earth Planet. Inter. **79**, 195–218 (1993).
17. H. Downes, A. D. Beard, K. Jarvis, and V. Vetrin, "Mantle Xenoliths from the Kola Peninsula: Evidence for Mantle Processes beneath the Baltic Shield," in *Proceedings of 5th Workshop of the SVEKALAPKO Project, Lammi, Finland, 2000* (Lammi, 2000), p. 15.
18. H. Downes, P. Peltonen, I. Mänttäri, and E. V. Sharkov, "Proterozoic Zircon Ages from Lower Crustal Granulite Xenoliths, Kola Peninsula, Russia: Evidence for Crustal Growth and Reworking," J. Geol. Soc. **159**, 485–488 (2002).
19. G. Faure, *Principles in Isotope Geology* (Wileys, New York, 1986; Mir, Moscow, 1989).
20. T. Frisch, G. D. Jackson, V. A. Glebovitsky, et al., "U–Pb Ages of Zircon from the Kolvitsa Gabbro–Anorthosite Complex, Southern Kola Peninsula, Russia," Petrologiya **3** (3), 248–254 (1995) [Petrology **3** (3), 219–225 (1995)].
21. *Geology of the Kola Peninsula*, Ed. by F. P. Mitrofanov (Kola Sci. Centre, Apatite, 1995).
22. V. A. Glebovitsky, "Tectonics and Regional Metamorphism of the Early Precambrian of the Eastern Baltic Shield," Reg. Geol. Metallogen., No. 1, 7–24 (1993).
23. S. J. Goldstein and S. B. Jacobsen, "Nd and Sr Isotopic Systematics of River Water Suspended Material: Implications for Crustal Evolution," Earth Planet. Sci. Lett. **87**, 249–265 (1988).
24. M. Grad and U. Luosto, "Seismic Models of the Crust of the Baltic Shield along the SVEKA Profile in Finland," Ann. Geophys., No. 5, 639–650 (1987).
25. *Greenstone Belts of the East European Platform Basement* (Nauka, Leningrad, 1988) [in Russian].
26. P. Hölttä, H. Huhma, I. Mänttäri, et al., "Petrology and Geochemistry of Mafic Granulite Xenoliths from the Lahtojoki Kimberlite Pipe, Eastern Finland," Lithos **51**, 109–133 (2000).
27. *Imandra–Varzuga Karelide Zone: Geology, Geochemistry, and Evolution* (Nauka, Leningrad, 1982) [in Russian].
28. B.-M. Jahn, F. Wu, and B. Chen, "Massive Granitoid Generation in Central Asia: Nd Isotope Evidence and Implication for Continental Growth in the Phanerozoic," Episodes **23** (2), 82–92 (2000).
29. P. D. Kempton, H. Downes, E. V. Sharkov, et al., "Petrology and Geochemistry of Xenoliths from the Northern Baltic Shield: Evidence for Partial Melting and Metasomatism in the Lower Crust beneath an Archaean Terrane," Lithos **36**, 157–184 (1995).
30. P. D. Kempton, H. Downes, L. A. Neymark, et al., "Garnet Granulite Xenoliths from the Northern Baltic Shield—the Underplated Lower Crust of a Palaeoproterozoic Large Igneous Province?," J. Petrol. **42** (4), 731–763 (2001).
31. V. N. Kobranova, B. I. Izvekov, S. L. Patsevich, and M. D. Shvartsman, *Determination of Petrophysical Characteristics on Samples* (Nauka, Moscow, 1977) [in Russian].
32. K. Condie, *Archean Greenstone Belts* (Elsevier, Amsterdam, 1981; Mir, Moscow, 1983).
33. M. Yu. Koreshkova, L. K. Levskii, and V. V. Ivanikov, "Petrology of a Lower Crustal Xenolith Suite from Dikes and Explosion Pipes of the Kandalaksha Graben," Petrologiya **9** (1), 89–106 (2001) [Petrology **9** (1), 79 (2001)].
34. U. Kramm, L. N. Kogarko, V. A. Kononova, and H. Vartiainen, "The Kola Alkaline Province of the CIS and Finland: Precise Rb–Sr Ages Define 380–360 Ma Age Range for All Magmatism," Lithos **30**, 33–44 (1993).
35. A. A. Kremenetskii and L. N. Ovchinnikov, *Geochemistry of the Deep-Seated Rocks* (Nauka, Moscow, 1986) [in Russian].
36. A. A. Kremenetskii, *Metamorphism of Precambrian Mafic Rocks* (Nauka, Moscow, 1979) [in Russian].
37. R. Kretz, "Symbols for Rock-Forming Minerals," Am. Mineral. **68**, 277–279 (1983).
38. I. T. Kukkonen and P. Peltonen, "Xenolith-Controlled Geotherm for the Central Fennoscandian Shield: Implication for Lithosphere–Asthenosphere Relations," J. South Am. Earth Sci. **304**, 301–315 (1999).
39. T. S. Lebedev, V. A. Korchin, B. Ya. Savenko, et al., *High-Pressure Petrophysical Studies and Their Geophysical Implications* (Naukova Dumka, Kiev, 1988) [in Russian].
40. T. C. Liew and A. W. Hofmann, "Precambrian Crustal Components, Plutonic Associations, Plate Environment of the Hercynian Fold Belt of Central Europe: Indications from a Nd and Sr Isotopic Study," Contrib. Mineral. Petrol. **98** (2), 129–138 (1988).
41. S. B. Lobach-Zhuchenko, N. A. Arestova, V. P. Chekulaev, et al., "Geochemistry and Petrology of 2.40–2.45 Ga Magmatic Rocks in the North-Western Belomorian Belt, Fennoscandian Shield, Russia," Precambrian Res. **92**, 223–250 (1998).
42. S. B. Lobach–Zhuchenko, V. P. Chekulaev, V. S. Stepanov, et al., "The White Sea Foldbelt—Late Archean Accretion- and Collision-related Zone of the Baltic Shield," Dokl. Akad. Nauk **358** (2), 226–229 (1998) [Dokl. Earth Sci. **358** (1), 34 (1998)].
43. A. J. W. Markwick and H. Downes, "Lower Crustal Granulite Xenoliths from the Arkhangelsk Kimberlite Pipes: Petrological, Geochemical and Geophysical Results," Lithos **51**, 135–151 (2000).
44. V. A. Melezhik and B. A. Sturt, "General Geology and Evolutionary History of the Early Proterozoic Polmak–Pasvik–Pechenga–Imandra–Varzuga–Ust'Ponoy Greenstone Belt in the Northeastern Baltic Shield," Earth Sci. Rev. **36**, 205–241 (1994).
45. R. I. Mil'kevich, Yu. V. Miller, V. A. Glebovitsky, et al., "Tholeiitic and Calc-Alkaline Magmatism in the North-

ern Part of the Tikshozero Greenstone Belt: Geochemical Evidence of a Subduction Environment," Geokhimiya, No. 12, 1262–1274 (2003) [Geochem. Int. **41** (12), 1152 (2003)].

46. M. V. Mints, V. N. Glaznev, A. N. Konilov, et al., *Early Precambrian of the Northeastern Baltic Shield: Paleogeodynamics, Structure, and Evolution of the Continental Crust* (Nauchnyi Mir, Moscow, 1996) [in Russian].
47. F. P. Mitrofanov, A. A. Zhangurov, Zh. A. Fedotov, et al., "Platinum Potential of the Imandra Layered Intrusion," in *Platinum of Russia* (Geoinformmark, Moscow, 1995), pp. 26–42 [in Russian].
48. F. P. Mitrofanov, V. V. Balaganskii, Yu. A. Balashov, et al., "U–Pb Age of Gabbro–Anorthosites of the Kola Peninsula," Dokl. Akad. Nauk **333** (1), 95–98 (1993).
49. S. Moorbath and P. N. Taylor, "Geochronology and Related Isotope Geochemistry of High-Grade Metamorphic Rocks from the Lower Continental Crust," Geol. Soc. Spec. Publ. **24**, 211–220 (1986).
50. L. A. Neymark, A. A. Nemchin, V. R. Vetrin, and E. A. Sal'nikova, "Sm–Nd and Pb–Pb Isotope Systems in the Lower Crustal Xenoliths from Dikes and Explosion Pipes in the Southern Kola Peninsula," Dokl. Akad. Nauk **329** (6), 781–784 (1993).
51. R. C. Newton and D. Perkins, "Thermodynamic Calibration of Geobarometers Based on the Assemblages Garnet–Plagioclase–Orthopyroxene (Clinopyroxene)–Quartz," Am. Mineral. **67**, 203–222 (1982).
52. P. Peltonen, K. A. Kinnunen, and H. Huhma, "Petrology of Two Diamondiferous Eclogite Xenoliths from the Lahtojoki Kimberlite Pipe, Eastern Finland," Lithos **63**, 151–164 (2002).
53. *Petrophysical Characteristics of the Russian Baltic Shield* (Kol'sk. Fil. AN SSSR, Apatity, 1976) [in Russian].
54. R. Powell and T. J. B. Holland, "An Internally Consistent Data Set with Uncertainties and Correlations: 3. Applications to Geobarometry, Worked Examples and a Computer Program," J. Metamorph. Geol. **6**, 173–204 (1988).
55. R. Powell, "Regression Diagnostics and Robust Regression in Geothermometer/Geobarometer Calibration: the Garnet–Clinopyroxene Geothermometer Revisited," J. Metamorph. Geol. **3**, 327–342 (1985).
56. *Precambrian Volcanism and Sedimentation in the Northeastern Baltic Shield* (Nauka, Leningrad, 1987) [in Russian].
57. A. A. Predovskii, *Reconstruction of the Settings of Early Precambrian Sedimentation and Volcanism* (Nauka, Leningrad, 1980) [in Russian].
58. N. M. S. Rock, *Lamprophyres* (Blackie, Glasgow, 1991).
59. R. L. Rudnick and D. M. Fountain, "Nature and Composition of the Continental Crust: a Lower Crustal Perspective," Rev. Geophys. **33** (3), 267–309 (1995).
60. A. V. Savitskii, V. I. Stepanenko, E. B. Anderson, et al., "New Data on the Granites of the Southwestern Kola Peninsula," Dokl. Akad. Nauk SSSR **302** (5), 1186–1191 (1988).
61. E. V. Sharkov and I. S. Puchtel, "Mineralogy of Eclogites (Garnet Websterites) and Eclogite-like rocks from the Explosion Pipes of Elovy Island, Kola Peninsula," in *Deep-seated Xenoliths and Lithospheric Structure* (Nauka, Moscow, 1987), pp. 127–148 [in Russian].
62. E. V. Sharkov, G. A. Snyder, L. A. Taylor, and T. F. Zinger, "An Early Proterozoic Large Igneous Province in the Eastern Baltic Shield: Evidence from the Mafic Drusite Complex, Belomorian Mobile Belt, Russia," Intern. Geol. Review **41**, 73–93 (1999).
63. E. V. Sharkov, I. S. Krassivskaya, and A. V. Chistyakov, "Dispersed Mafic–Ultramafic Intrusive Magmatism in Early Paleoproterozoic Mobile Zones of the Baltic Shield: An Example of the Belomorian Drusite (Coronite) Complex," Petrologiya **12** (6), 632–655 (2004) [Petrology **12** (6), 561 (2004)].
64. N. V. Sharov, *Lithosphere of the Baltic Shield Based on Seismic Data* (Kol'sk. Nauch. Ts. Ross. Akad. Nauk, Apatity, 1993) [in Russian].
65. K. A. Shurkin and T. A. Rumyantseva, *Explosion Breccia of the Kandalaksha Alkaline Lamprophyre Complex. Petrologic–Mineralogic Features of the Rocks and Technical Stones* (Nauka, Moscow, 1979) [in Russian].
66. V. F. Smolkin, V. V. Borisova, S. A. Svetov, and A. E. Borisov, "Late Archean Komatiites of the Ura Bay–Titovka Structure, Northwestern Kola Region," Petrologiya **8** (2), 199–224 (2000) [Petrology **8** (2), 177 (2000)].
67. V. F. Smolkin, Zh. A. Fedotov, Yu. N. Neradovskii, et al., *Layered Intrusions of the Monchegorsk Ore District: Petrology, Mineralization, Isotopy, and Deep-Seated Structure* (Kol'sk. Nauch. Tsentr, Apatity, 2004), Part 2 [in Russian].
68. V. S. Stepanov, *Precambrian Mafic Magmatism of the Western Belomorian Region* (Nauka, Leningrad, 1981) [in Russian].
69. S.-S. Sun and W. F. McDonough, "Chemical and Isotopic Systematics of Oceanic Basalts: Implications for Mantle Composition and Processes," in "Magmatism in the Ocean Basins," Ed. by M. J. Norry, Geol. Soc. London Spec. Publ. **42**, 313–345 (1989).
70. E. N. Terekhov and V. I. Levitskii, "Granulites of the Lapland Belt: Rare-Earth Elements and Petrogenetic Problems," Izv. Vyssh. Uchebn. Zaved., Geol. Razved., No. 5, 3–18 (1993).
71. M. J. Timmerman and J. S. Daly, "Sm–Nd Evidence for Late Archaean Crust Formation in the Lapland–Kola Mobile Belt, Kola Peninsula, Russia and Norway," Precambrian Res. **72**, 97–107 (1995).
72. A. A. Tripol'skii and N. V. Sharov, *Lithosphere of the Precambrian Shields in the Earth's Northern Hemisphere Based on Seismic Data* (Karel'sk. Nauch. Tsentr Ross. Akad. Nauk, Petrozavodsk, 2004) [in Russian].
73. V. R. Vetrin and A. A. Nemchin, "The U–Pb Age of Zircon from a Granulite Xenolith in the Diatreme on the Elovy Island, the Southern Kola Peninsula," Dokl. Akad. Nauk **359** (6), 808–810 (1998) [Dokl. Earth Sci. **359A** (3), 454 (1998)].
74. V. R. Vetrin and A. V. Travin, "Age of the Modal Metasomatism during the Formation of the Paleozoic Kola Alkaline Province," in *Proceedings of the 21st All-Russia Seminar and School on the Earth's Alkaline Magmatism. Geochemistry of the Magmatic Rocks, Apatity, Russia, 2003* (Kol'sk. Nauch. Tsentr, Ross. Akad. Nauk, Apatity, 2003), pp. 36–38 [in Russian].
75. V. R. Vetrin and M. M. Kalinkin, *Reconstruction of Crustal and Crustal–Mantle Magmatism and Metasom-*

*atism* (Kol'sk. Nauch. Tsentr, Ross. Akad. Nauk, Apatity, 1992) [in Russian].

76. V. R. Vetrin, "Lower Crust of the Belomorian Megablock: Age, Composition, and Formation Conditions (Evidence from Deep-seated Xenoliths)," Vestn. Murmansk. Gos. Tekhn. Univ. **1** (3), 53–60 (1998).
77. V. R. Vetrin, T. B. Bayanova, I. L. Kamenskii, and S. V. Ikorskii, "U–Pb Ages and Helium Isotope Geochemistry of Rocks and Minerals from the Litsk–Araguba Diorite–Granite Complex (Kola Peninsula)," Dokl. Akad. Nauk **386** (2), 85–89 (2002) [Dokl. Earth Sic. **387** (8), 947 (2002)].
78. O. I. Volodichev, *Belomorian Belt of Karelia (Geology and Petrology)* (Nauka, Leningrad, 1990) [in Russian].
79. A. B. Vrevsky, V. A. Matrenichev, and M. S. Ruzh'eva, "Petrology of Komatiites from the Baltic Shield and Isotope Geochemical Evolution of Their Mantle Sources," Petrologiya **11** (6), 587–617 (2003) [Petrology **11** (6), 532 (2003)].